

*Author for Correspondence: Anne D. Yoder, Department of Biology, Duke University,
Durham, USA, 919-660-7366, anne.yoder@duke.edu

Keywords (6): speciation, pheromone receptors, synteny, gene family evolution, nocturnality,
vomeronasal

4 **Abstract**

5 Sensory gene families are of special interest, both for what they can tell us about
6 molecular evolution, and for what they imply as mediators of social communication. The
7 vomeronasal type-1 receptors (V1Rs) have often been hypothesized as playing a fundamental
8 role in driving or maintaining species boundaries given their likely function as mediators of
9 intraspecific mate choice, particularly in nocturnal mammals. Here, we employ a comparative
10 genomic approach for revealing patterns of V1R evolution within primates, with a special focus
11 on the small-bodied nocturnal mouse and dwarf lemurs of Madagascar (genera *Microcebus* and
12 *Cheirogaleus*, respectively). By doubling the existing genomic resources for strepsirrhine
13 primates (i.e., the lemurs and lorises), we find that the highly-speciose and morphologically-
14 cryptic mouse lemurs have experienced an elaborate proliferation of V1Rs that we argue is
15 functionally related to their capacity for rapid lineage diversification. Contrary to a previous
16 study that found equivalent degrees of V1R diversity in diurnal and nocturnal lemurs, our study
17 finds a strong correlation between nocturnality and V1R elaboration, with nocturnal lemurs
18 showing elaborate V1R repertoires and diurnal lemurs showing less diverse repertoires.
19 Recognized subfamilies among V1Rs show unique signatures of diversifying positive selection,
20 as might be expected if they have each evolved to respond to specific stimuli. Further, a detailed
21 syntenic comparison of mouse lemurs with mouse (genus *Mus*) and other mammalian outgroups
22 shows that orthologous mammalian subfamilies, predicted to be of ancient origin, tend to cluster
23 in a densely populated region across syntenic chromosomes that we refer to as V1R “hotspots.”
24

25 **Introduction**

26 The evolutionary dynamics of sensory gene families are of fundamental interest as a
27 model for how molecular evolutionary processes can shape the content and structure of genomes
28 and for their ability to characterize the life history and ecological traits of organisms.

29 Vomeronasal type-1 receptor genes (V1Rs) comprise one such gene family and have been the
30 subject of increasing interest in both the molecular genetics (e.g., Adipietro et al. 2012) and
31 evolutionary genetics (e.g., Yohe and Brand 2018) communities. Vomeroolfaction is a form of
32 chemosensation that mediates semiochemical detection and occurs in the vomeronasal organ
33 (VNO) of mammals (Leinders-Zufall et al. 2000). V1Rs are expressed on vomeronasal sensory
34 neurons in the VNO and have been demonstrated to detect pheromones in mice (Boschat et al.
35 2002; Haga-Yamanaka et al. 2014). For example, impaired vomeronasal function in mice, either
36 through a knockout of V1Rs or removal of the VNO, alters appropriate chemosensory behaviors
37 such as conspecific avoidance of sick animals, interspecies defensive cues, male sexual behavior,
38 and maternal aggression (Del Punta et al. 2002; Papes et al. 2010; Boillat et al. 2015). Thus, the
39 evolution of V1Rs can have direct consequences for both the emitter and the receiver of
40 pheromone signals, with ample evidence indicating that molecular evolution of V1Rs is
41 associated with the speciation process (Lane et al. 2002; Kurzweil et al. 2009; Hohenbrink et al.
42 2012; Nikaido et al. 2014).

43 V1Rs are ideally suited for study within the context of "sensory drive" wherein mate
44 preferences in communication systems diverge in the face of novel environmental opportunity
45 (Boughman 2002). Communication mechanisms for mate recognition have been recognized as
46 an important component for driving rapid reproductive isolation (Mendelson 2003; Dopman et
47 al. 2010; Servedio and Boughman 2017; Brand et al. 2019) and with the reinforcement of species

48 boundaries (Servedio and Noor 2003). Sensory drive can affect diverging populations in two
49 ways by targeting the pheromone receptors and/or their signaling molecules. As examples,
50 adaptation of a likely V1R signal in mice, androgen binding protein, is associated with
51 assortative mating between *Mus musculus* subspecies (Karn et al. 2010; Chung et al. 2017; Hurst
52 et al. 2017) just as fixation of nonsynonymous polymorphisms among V1Rs is associated with
53 the speciation of *Mus spretus* and *Mus musculus* (Kurzweil et al. 2009). Moreover, it has been
54 shown that differential expression of vomeronasal and olfactory receptor genes, including V1Rs,
55 is associated with assortative mating in a pair of house mouse subspecies (Loire et al. 2017) and
56 is likely reinforcing the subspecies along their hybrid zone.

57 The V1R gene family has experienced many duplications and losses in the evolutionary
58 history of mammals, and the availability of duplicate copies can allow for divergence among
59 sequences, gene expression, and ultimately function (e.g. Lynch and Conery 2000; Des Marais
60 and Rausher 2008). Though not directly addressed in this study, it is worth noting that changes in
61 gene expression often occur rapidly after gene duplication events (Makova and Li 2003; Keller
62 and Yi 2014; Guschanski et al. 2017) and are often accompanied by shifts in rates of molecular
63 evolution (Chen et al. 2010; Yang and Gaut 2011). Although the mechanisms that explain
64 variable rates of molecular evolution, specifically the nonsynonymous to synonymous
65 substitution rate ratio (dN/dS), are complex, there is some interdependence on expression levels
66 (O'Toole et al. 2018) and genome architecture (Dai et al. 2014; Xie et al. 2016). The V1R gene
67 family demonstrates structural complexity (Ohara et al. 2009; Yohe et al. 2018), and gene family
68 expansions and directional selection acting on duplicate copies may be important for the
69 maintenance of species boundaries where vomerolfaction is linked with assortative mating (Luo
70 et al. 2003; Isogai et al. 2011; Fu et al. 2015).

71 Here, we present a comparative genomic study of V1R evolution within the lemuriform
72 primates, primarily focusing on the mouse lemurs of Madagascar (genus *Microcebus*). Mouse
73 lemurs are perhaps the most species-rich clade of living primates (Hotaling et al. 2016), and are
74 well-known for high levels of interspecific genetic divergence though with nearly uniform
75 morphological phenotypes. They have thus come to be regarded as a classic example of a
76 cryptic species radiation, perhaps related to their nocturnal lifestyle (Yoder et al. 2016). Mouse
77 lemurs, and the closely-related dwarf lemurs, have elaborate olfactory communication behaviors
78 that are associated with adaptive strategies such as predator recognition (Sündermann et al.
79 2008), fecundity (Drea 2015), and even biased sex ratios (Perret 1996; Perret and Colas 1997).
80 V1Rs take on particular interest in mouse lemurs as we hypothesize that their observed role in
81 both speciation and in the maintenance of species boundaries within *Mus* may also apply to this
82 speciose clade of primates (Smadja et al. 2015; Loire et al. 2017). We hypothesize that among
83 primates, mouse lemurs will show signatures of sensory drive via genomic elaboration of the
84 V1R complex and evidence of positive selection acting on V1R genes.

85 There are numerous lines of evidence to lead us to this hypothesis: 1) Previous studies
86 have indicated that V1Rs within the lemuriform clade have evolved under pervasive positive
87 selection 5/22/19 3:35:00 PM, 2) that the majority of gene copies are intact (Young et al. 2010;
88 Larsen et al. 2014), and 3) that the differential expression of a large number of vomeronasal
89 receptors in both the VNO and main olfactory epithelium of mouse lemurs are associated with
90 different behaviors and chemical signals (Hohenbrink et al. 2014). In fact, along with murids,
91 opossums, and platypus, mouse lemurs have been reported to have among the largest V1R
92 repertoires found in mammals (Young et al. 2010). Even so, numerous obstacles such as
93 complexities of chemical background, chemical signals, and the genetic basis of chemosensation

94 complicate both ecological and experimental approaches for differentiating between cause and
95 effect in the speciation process (Yohe and Brand 2018). This is particularly problematic for
96 studies of mouse lemurs given their remote geographic distribution, nocturnal life history, and
97 endangered status. Thus, we take a comparative genomic approach for reconstructing the
98 evolutionary dynamics of the V1R gene family within the small-bodied and nocturnal mouse and
99 dwarf lemurs (family, Cheirogaleidae).

100

101 **A Comparative Genomic Approach**

102 V1R loci are highly repetitive and they, along with their surrounding regions, are
103 notoriously challenging for genome assembly. Though previous studies have used targeted
104 sequencing or short-read sequencing to examine the evolutionary dynamics of V1R expansions
105 in a limited number of species (Young et al. 2010; Hohenbrink et al. 2012; Yoder et al. 2014),
106 strepsirrhine primates have until recently remained woefully underrepresented in genomic
107 databases (Perry et al. 2012; Meyer et al. 2015; Larsen et al. 2017; Hawkins et al. 2018). Here,
108 we take advantage of the chromosome-level assembly of the gray mouse lemur, *Microcebus*
109 *murinus*, along with short-read sequencing in related species, to characterize the V1R repertoires
110 for lemuriform primates. Recent improvements using long-read sequencing of the mouse lemur
111 genome (Larsen et al. 2017) improve our ability to characterize the V1R repertoire (Larsen et al.
112 2014) and allow for comparisons of the genomic architecture of V1R-containing regions in
113 expanded and contracted V1R repertoires across mammals.

114 In this study, we have sequenced and assembled seven new cheirogaleid genomes, with a
115 particular focus on the mouse lemurs. Further, to explore intraspecific copy number variation and
116 evaluate the effects of assembly error on V1R repertoire counts, we resequenced and *de novo*

117 assembled genomes from eight *M. murinus* individuals from a captive breeding colony. Our
118 study thus serves as a timely companion to two recent overviews of comparative genomic studies
119 for illuminating the evolutionary and life-history dynamics of chemosensory gene family
120 evolution in vertebrates (Bear et al. 2016; Hughes et al. 2018). A comparative genomic approach
121 allows us to explore classic predictions of gene-family evolution, namely, that genomic drift can
122 operate at very fine scales to produce high intraspecific copy number variation (Nozawa et al.
123 2007) and that gene-family evolution is often marked by a strong birth-death process over
124 phylogenetic time scales (Nei et al. 1997; Csűrös and Miklos 2009; Hughes et al. 2018). The
125 latter question is of particular interest for V1R evolution given that adaptive pressures on these
126 genes makes them highly vulnerable to pseudogenization in cases of relaxed selection, thus
127 yielding the observed correlations between levels of V1R ornamentation and diverse adaptive
128 regimes. An overview of primates shows that those with elaborate representation of subfamilies
129 have a strong reliance on chemosensory communication whereas those with depauperate V1R
130 representation rely on alternative mechanisms for inter- and intra-specific communication (Yoder
131 and Larsen 2014).

132 These new genomic resources have also allowed us to address a number of questions
133 regarding rates of molecular evolution in V1Rs. Divergent gene function following gene
134 duplication predicts that some signature of positive selection should be evident in the gene
135 sequences (Zhang et al. 1998), but it remains unknown if selection has acted pervasively over
136 time or has occurred in episodic bursts prior to the diversification of mouse lemurs. We might
137 anticipate episodic positive selection to be the primary mechanism if purifying selection has been
138 operating at more recent time scales to preserve gene function among duplicate copies. For
139 strepsirrhine primates (i.e., the lemurs and lorises), pervasive positive selection has been detected

140 at the interspecific level (Hohenbrink et al. 2012; Yoder et al. 2014), while strong purifying
141 selection has been found within populations. Here we disentangle pervasive versus episodic
142 positive selection among V1Rs and show that both gene duplication and rates of molecular
143 evolution have been active in shaping expanded V1R repertoires among the dwarf and mouse
144 lemurs. Moreover, through comparison with *Mus* and other mammals, we show that orthologous
145 subfamilies tend to cluster in a densely populated region on syntenic chromosomes that we refer
146 to as V1R "hotspots."

147

148 **Results and Discussion**

149 **Novel genome assemblies of several strepsirrhine primates**

150 *We de novo* assembled seven novel strepsirrhine genomes: *Microcebus griseorufus*, *M.*
151 *ravelobensis*, *M. mittermeieri*, *M. tavaratra*, *Mirza zaza*, *Cheirogaleus sibreei* and *C. medius*.
152 These efforts have doubled the number of publicly available genomes for the Strepsirrhini with a
153 specific focus on the dwarf and mouse lemur clade. Excluding *C. medius*, the seven genomes
154 were sequenced to an average depth of coverage between 26x and 45x with scaffold N50s of 17-
155 76kb (Supplementary Table S1). The *C. medius* reference genome was assembled using Dovetail
156 Genomics to an average depth of coverage of 110x and a scaffold N50 of approximately 50Mb
157 (Williams et al. 2019). We evaluated assembly completeness using the Benchmarking Universal
158 Single-Copy Orthologs tool, BUSCO (Simão et al. 2015), which assesses genomes for the
159 presence of complete near-universal single-copy orthologs (Supplementary Figure S1). The
160 assemblies recovered between 77.2% and 92.3% of the mammalian BUSCO gene set. We also
161 resequenced eight *M. murinus* individuals, with one duplicate individual (Campbell et al. 2019),
162 and here have *de novo* assembled genomes for each individual with 21x-29x effective coverage

163 using the 10x Genomics Supernova pipeline. The additional scaffolding information provided by
164 the 10x Genomics linked-reads resulted in scaffold N50s of 0.6-1.2 Mb. BUSCO analyses
165 revealed that the resequenced assemblies recovered between 89.9% and 95.5% of the
166 mammalian gene set. A denser sampling of genomes within Cheirogaleidae not only provides an
167 opportunity for illuminating patterns of V1R gene family evolution but also promotes greater
168 understanding of the molecular evolution of primate and strepsirrhine-specific genomes. Genome
169 resequencing of *M. murinus* individuals has allowed investigation of intraspecific V1R copy
170 number variation as well as questions regarding microevolutionary processes and gene family
171 evolution (Park et al. 2011).

172 The monophyletic genus *Microcebus* contains 24 named species (Hotaling et al. 2016),
173 and our results clearly demonstrate that the clade has a uniquely complex V1R repertoire
174 compared to other primates thus far characterized (Figure 1A and B). Contrary to a previous
175 study suggesting that V1R expansion is ubiquitous across the lemuriform clade (Yoder et al.
176 2014), increased sampling reveals that expansion has been profound in the nocturnal dwarf and
177 mouse lemurs. This is consistent with the original hypothesis that local V1R expansions may
178 play a role in forming or maintaining speciation boundaries within *Cheirogaleus* and *Microcebus*
179 as might be predicted given their nocturnal lifestyle. Phylogenetic analyses revealed that
180 expanded V1R repertoires in mouse lemurs demonstrate a remarkably higher rate of duplicate
181 gene retention in comparison to other primates (Figure 1A and B; Table 1). The common
182 ancestor of mouse lemurs is not associated with novel subfamily birth though the diversity and
183 number of V1R gene copies is striking (Figure 1A; Table 1). Although genomes generated
184 exclusively from short-read data are vulnerable to collapsing loci in assemblies (Larsen et al.
185 2014), our inference of increased V1R retention in *M. murinus* relative to non-cheirogaleid

186 primates was robust to assembly strategies and data sources (Supplementary Table S2). Further,
187 the resequenced *M. murinus* individuals reveal low intraspecific variation in copy number
188 (Figure 2), suggesting that the observed differences in repertoire size between mouse lemurs and
189 other non-nocturnal lemurs is not an artifact of individual sampling or assembly error (Figure 3).

190 The expansion dynamics of V1Rs within Cheirogaleidae do not support a simple linear
191 correlation between species richness and repertoire size. Although all cheirogaleid repertoires
192 had full primate subfamily membership, there was variation in subfamily proportions between
193 species, which is consistent with our hypothesis that species-specific V1R repertoires and
194 chemosensation may be important for species diversity of cheirogaleids in comparison to diurnal
195 strepsirrhines. Dwarf lemurs, genus *Cheirogaleus*, are hypothesized to have as many as 18
196 species (Lei et al. 2014) though have the smallest V1R repertoires within the cheirogaleids
197 examined here. Conversely, the genus *Mirza*, with only two recognized species, has a repertoire
198 size that is nearly equal to that of *Microcebus murinus*. It is notable, however, that the *Mirza*
199 genome's expanded repertoire is primarily enriched for subfamily III (Figure 1A). The
200 differential subfamily enrichment among species suggests that despite the similarity in size to
201 *Microcebus* repertoires, the V1R repertoire of *Mirza* has experienced independent selective
202 pressures on gene retention and may ultimately fulfill a different functional role compared to
203 *Microcebus*.

204

205 **V1R repertoire estimation across primates**

206 We estimated V1R repertoire size evolution across strepsirrhine primates as well as for
207 several well-annotated primate and mammalian genomes for outgroup comparison. Notably,
208 repertoire estimates of extant primates are comparable to previous studies that used trace archive

209 fragments and earlier draft genome versions (Figure 3; Supplemental Table S2; Young et al.
210 2010; Moriya-Ito et al. 2018). The expanded V1R repertoire within the gray mouse lemur is not
211 ubiquitous across the Strepsirrhini, however. Rather, repertoire size expanded gradually from a
212 reduced set in the strepsirrhine common ancestor to its peak in the mouse lemur clade. This
213 expansion is characterized by a reduced repertoire in the early diverging aye-aye lineage (genus
214 *Daubentonia*), moderate repertoires among diurnal lemurs, and an expansion that likely occurred
215 in the common ancestor of Cheirogaleidae (Figure 3). If the origins of many V1R copies in
216 mouse lemur date to the Cheirogaleidae common ancestor, this means that at least some of those
217 duplicates have remained functional and intact since their origins 30 million years ago, as would
218 be consistent with divergence time estimates for the cheirogaleid radiation (Yang and Yoder
219 2003; dos Reis et al. 2018).

220 Within Cheirogaleidae, repertoire sizes ranged from a low of 58 intact V1Rs in *C. medius*
221 to highs between 102-143 intact V1Rs in the genus *Microcebus*. The mouse lemurs have
222 universally large V1R repertoires (102-146 intact genes) with notable intragenus variation. Prior
223 to this study, *M. murinus* had been identified as having one of the largest V1R repertoires within
224 mammals (Young et al. 2010). Additional sampling from *Microcebus* reveals, however, that
225 among the five mouse lemur species here characterized, *M. murinus* actually has the smallest
226 repertoire with only 102 intact V1Rs. We also estimated the percent of intact V1Rs contained
227 within the total repertoire for each species. Most haplorrhine primates (Anthropoidea plus
228 *Tarsius*) species have repertoires with low percentages of intact receptors (<37% intact). Within
229 Lemuroidea, the diurnal lemurs also have small and pseudogenized repertoires (26% to 49%
230 intact) containing only 22-27 intact V1Rs. In contrast, among nocturnal species excluding aye-

231 aye, we observe intact repertoires between 58% to 66% within Cheirogaleidae, and 61% for the
232 nocturnal loriform *Otolemur garnetti*.

233 These comparisons do not, however, provide definitive evidence that expanded V1R
234 repertoires in primates are strictly associated with nocturnal life history (Wang et al. 2010;
235 Moriya-Ito et al. 2018). Although *Otolemur garnetti* shows a proportion of intact V1R copies
236 similar to dwarf and mouse lemurs (Figure 3), subfamilies VII and IX are absent from *O.*
237 *garnetti* (Figure 1B). By comparison, the genomes of both the aye-aye and the tarsier (Schmitz et
238 al. 2016) contain low numbers of intact V1R gene copies, which appears to contradict the
239 hypothesis that a nocturnal life history alone is sufficient for explaining V1R elaboration in
240 mouse lemurs. Though it is true that both aye-aye and tarsier have more V1R copies than the
241 diurnal primates compared here, they also show a high proportion of putative pseudogenes and
242 an absence of some V1R subfamilies found in Cheirogaleidae (Figure 1A and B).

243 Our phylogenetic approach reveals a pattern of gene family evolution compatible with
244 active gene birth and death (Nei et al. 1997; Csűrös and Miklos 2009; Hughes et al. 2018) with
245 an independent V1R expansion isolated to Cheirogaleidae with three subfamily gains rather than
246 a single more ancient expansion followed by losses in diurnal lineages (Table 1). Although the
247 gain and loss dynamics of V1Rs over time is complex with uncertainty in the origins of specific
248 subfamilies, variation in subfamily membership among species suggests that nocturnal primates
249 possess more diverse repertoires than their diurnal counterparts (Figure 1A and B). These results
250 are suggestive of an association between nocturnal life histories and V1R repertoire evolution, as
251 well as the importance of chemosensation generally among nocturnal primates. Our findings are
252 not conclusive, however, as the pattern observed in aye-aye deviates from this expectation,
253 though it must be noted that the quality of the aye-aye genome assembly is considerably poorer

254 than the others compared with the lowest contig/scaffold N50 and most incomplete BUSCO
255 results (Supplementary Figure S1 and Table S1). An improved genome for aye-aye, a notably
256 solitary primate (Sterling and Richard 1995), as well as genomes for species within the diurnal
257 nest-dwelling genus, *Varecia*, will allow for more formal tests of how life history traits are
258 correlated with V1R copy number.

259
260

261 **Subfamily membership and ancestral repertoire reconstruction**

262

263 For each genome analyzed, we classified repertoire subfamily membership based on
264 homology inferred from a maximum likelihood (ML) tree (Figure 4) and previously-described
265 subfamily designations (Hohenbrink et al. 2012). During alignment, sequences that introduced
266 excessive gaps to transmembrane regions were iteratively removed, resulting in alignments of
267 increasing conservatism (see Materials and Methods “V1R repertoire estimation and ancestral
268 count reconstruction”). We tested whether these varying alignments affected our estimates of
269 subfamily composition and found little impact. Regardless of the number of sequences removed
270 from the alignment, the relative proportions of subfamily membership within each species
271 remained constant (Supplementary Figure S2). Although topological errors may contribute to
272 uncertainty in gene count reconstructions, the ML tree shows 70% or greater bootstrap support
273 for 63% of nodes (Figure 4), with little additional improvement possible due to the limitations of
274 a single-exon gene family (Supplementary Table S3). Our results suggest that both the ancestral
275 primate and the ancestral lemur had repertoires more limited in size and diversity than many
276 living strepsirrhine primates, further supporting the controversial hypothesis that the ancestral
277 primate was diurnal rather than nocturnal (Tan et al. 2005; Borges et al. 2018).

278 Subfamily membership varies among the other extant strepsirrhines examined (Figure 1A
279 and B). While *Otolemur garnetti* contains a very diverse repertoire, it lacks subfamily VII and IX
280 membership. The diurnal lemurs lack receptors belonging to a few subfamilies, most consistently
281 IV, VIII, and IX. The basal lineage within the lemuriform radiation, *Daubentonia*
282 *madagascariensis*, lacks membership for most subfamilies, including *Strep*/I, II, IV, V, and VII.
283 Subfamily I, referred to as “V1R*strep*” in Yoder et al. (2014), is used synonymously here for
284 distinction from the mouse subfamily “I”. The repertoires of cheirogaleids are highly enriched
285 for subfamily III, V, and IX membership, while the diurnal lemurs are enriched for subfamilies
286 *Strep*/I, II, and III. In haplorrhine primates, repertoires contain only one or a few subfamilies.
287 Ancestral state reconstruction with asymmetric parsimony (Csűrös and Miklos 2009; Csűrös
288 2010) revealed that the stem primate possessed only a subset of now extant V1R subfamilies,
289 *Strep*/I, II, III, IV and VIII (Figure 1B). Subfamily IX has undergone a notable expansion in
290 Cheirogaleidae, but the aye-aye repertoire also contains members from subfamily IX thus,
291 subfamily IX is the only subfamily exclusive to nocturnal strepsirrhines, despite its absence in
292 *Otolemur garnetti* (Figure 1A and B).

293

294 **Copy number variation in intraspecific *Microcebus murinus* repertoires**

295

296 We resequenced eight *M. murinus* individuals of known pedigree from the colony at the
297 Duke Lemur Center in Durham, North Carolina. Using these genomes, we estimated
298 intraspecific variation in V1R repertoire size (Figure 2). For the eight resequenced *M. murinus*
299 individuals, we observed low levels of intraspecific V1R repertoire size variation relative to size
300 variation between taxonomic families with individual repertoires ranging from 86 to 105 intact
301 V1R loci. Though one might expect that levels of intraspecific variation in V1R repertoire size in

302 a captive population may be reduced relative to wild populations of *M. murinus*, the colony at the
303 Duke Lemur Center shows signs of admixture from two distinct evolutionary lineages, *M.*
304 *murinus* and *M. ganzhorni* (Larsen et al., 2017), presently recognized as distinct species
305 (Hotaling et al., 2016). Therefore, the intraspecific variation observed here may actually be
306 exaggerated, rather than reduced, which increases our confidence in the robustness of repertoire
307 size estimates among species through sampling of single individuals. To test for the potentially
308 confounding effects of sequencing and assembly error, one individual, DLC7033, was sequenced
309 twice as a technical replicate. The duplicate genome assemblies respectively contained 92 or 96
310 intact loci indicating that sequencing and assembly error likely play a measurable role in
311 generating variation among observed repertoire counts, though the effect appears to be modest.
312 Thus, taking the results of the pedigree analysis as largely accurate, this emphasizes the highly
313 dynamic nature of V1R repertoire size evolution, even over generational timescales.

314

315 **Complex history of diversifying positive selection in the dwarf and mouse lemurs**

316 Our results agree with previous studies in finding that selection has acted pervasively
317 across the V1R gene family over time (Hohenbrink et. al. 2012). Pervasive positive selection was
318 revealed for all subfamilies identified in this study, even when analyzing the genus *Microcebus*
319 alone (Supplementary Tables S4 and S5) and additional genome sequences for dwarf and mouse
320 lemurs have likely increased the power of the sites tests. For example, positive selection was not
321 evident for subfamily VII in a previous study limited to only *Microcebus murinus* (Hohenbrink
322 et al. 2012). Furthermore, some subfamilies have unique profiles of sites under selection (Figure
323 5). Although lineage-specific rate variation is a confounding factor in V1R gene family evolution

324 (Yoder et al. 2014), our analyses, spanning a range of taxon sampling schemes, show that our
325 ability to characterize the V1R selection profiles are robust to such rate variation (Figure 5).

326 We performed two different model comparisons to differentiate between hypotheses of
327 neutrality versus selection, and for the latter, for differentiating between the effects of rate
328 constancy versus heterogeneity among sites. The M7 and M8 model comparisons always
329 recovered more sites under selection than the more conserved M1a and M2a comparisons, but
330 individual sites under selection detected by Bayes empirical Bayes with M2a were subsets of
331 those detected by M8. Both model comparisons use likelihood ratio tests (LRTs) to detect
332 positive selection and assume dN/dS is constant across branches, but the M2a and M1a
333 comparison (Zhang et al. 2005) uses three finite mixtures of dN/dS while the M8 and M7
334 comparison (Yang et al. 2000) accounts for heterogeneity in dN/dS among nearly neutral sites
335 with a beta distribution. Tests of pervasive positive selection were also performed on data
336 realigned by subfamily, and similar estimates of proportions of sites under positive selection
337 suggested that our site models were not misled by alignment errors (Supplementary Tables S6
338 and S7). Most individual sites under positive selection are unique to different subfamilies
339 (Supplementary Figure S3) and reflect biases in selective pressures across different loop and
340 transmembrane domains (Supplemental Figure S4). However, some selection profiles were more
341 differentiated than others, such as *Strep*/I, II, V, and IX (Figure 5). The divergent selection
342 profiles among subfamilies leads us to interpret positive selection acting on V1R genes in
343 primates to be largely diversifying. Differentiated selection profiles among subfamilies are
344 explained by biases among transmembrane and loop domains (Supplementary Material;
345 Supplementary Figure S5; Supplementary Tables S8-S10).

346 Previous studies have indicated that extracellular loops have been primary targets of
347 positive selection in V1Rs (Hohenbrink et al. 2012), and our results agree with these findings.
348 Positive selection acting on extracellular loops two and three from Hohenbrink et al. (2012),
349 identified here simply as loops three and five respectively, is evident (Supplementary Figure S5).
350 These specific domains are probable regions where V1Rs bind to semiochemicals (Hohenbrink
351 et al. 2012). Our results also show the transmembrane domains themselves, whether directly or
352 by linkage, have also been under variable levels of positive selection (Supplementary Material;
353 Supplementary Table S8). We find limited evidence for an enriched number of sites under
354 positive selection in transmembrane domains four and five, and a depletion in transmembrane
355 domain three, which have been previously predicted to form the ligand binding pocket of V1Rs
356 (Kobilka et al. 1988; Pilpel and Lancet 1999; Palczewski et al. 2000; Yoder et al. 2014). These
357 results prompt us to hypothesize that pervasive diversifying positive selection has accompanied
358 selection for divergent function among V1R subfamilies, although additional evidence is needed
359 for hypothesis testing.

360 Branch-site models detected evidence of episodic positive selection in the evolution of all
361 V1R subfamilies except for lemur VIII (Supplementary Figure S6; Supplementary Table S11).
362 Tests of episodic positive selection across the V1R subfamilies in the house mouse have been of
363 little interest (Karn et al. 2010) and our tests of episodic selection here are generally not
364 associated with the expansion of V1Rs in dwarf and mouse lemurs. However, subfamily IX
365 would be a candidate for further investigation, given that it was the only subfamily to show
366 notable levels of episodic positive selection, and is the only subfamily specific to nocturnal
367 strepsirrhines. Further, many of the sites identified to be under positive selection correspond to
368 the previously identified ligand binding domains (Supplementary Figure S6, Supplementary

369 Table S12). Exploration of alternative topologies revealed that branches showing episodic
370 positive selection were likely not due to topological errors (Supplementary Material;
371 Supplementary Figure S6).

372

373 **Comparative evolution of V1R repertoires and genome architecture across Mammalia**

374 Here we take advantage of the recently published chromosome-level assembly for *M.*
375 *murinus* and other chromosome-level mammalian assemblies in an effort to identify genomic
376 features that are generally associated with V1R expansion. The molecular environment of V1Rs
377 is predicted to play a role in their regulation and has previously been studied only in mouse, rat,
378 and pig (Lane et al. 2002; Stewart and Lane 2007; Kambere and Lane 2009; Michaloski et al.
379 2011; Dinka and Le 2017). We compared the expanded V1R repertoires of mouse and mouse
380 lemur with the putatively contracted V1R repertoires of horse, cow, dog, and human. As
381 predicted from previous studies (Kambere and Lane 2007; Kambere and Lane 2009), enrichment
382 for repetitive LINE elements is associated with expansion of V1Rs in mammals (Supplementary
383 Figure S7). We find that mouse lemur V1Rs primarily cluster by subfamily at chromosomal
384 locations across the genome as is also characteristic of the V1R repertoire in mouse. Only mouse
385 lemur subfamily VIII does not form a cluster but is instead uniquely dispersed across three
386 different chromosomes (Figure 6). We also analyzed the locations of all regions demonstrating
387 V1R homology to determine if there are any potential pseudogenized subfamilies or clusters in
388 the genome and found no evidence for pseudogenized clusters of V1Rs in mouse lemur
389 (Supplemental Figure S12). Both LINE enrichment and physical clustering of V1R loci have
390 been predicted to be associated with proper regulation of V1Rs (Lane et al. 2002; Kambere and
391 Lane 2007) and may be characteristic of expanded V1R repertoires in general.

392 To investigate whether homologous subfamilies have retained chromosomal synteny in
393 species with expanded repertoires and across mammals broadly, we evaluated chromosomal
394 synteny for each species relative to mouse using the SynChro software (Drillon et al. 2014;
395 Figure 6, Figure 7A and B, Supplementary Figures S8-S11). In mouse and mouse lemur, most
396 homologous V1R subfamilies retain chromosomal synteny (Figure 6, Figure 7A and B). Mouse
397 subfamily D is most closely related to mouse lemur subfamily IV, and both subfamilies share
398 mouse chromosome 7 synteny. Subfamilies J/K and V as well as subfamilies G and *Strep*/I also
399 share mouse chromosome 7 synteny. Lemur subfamily III is syntenic with mouse E and F on
400 mouse chromosomes 6 and 7. Lemur subfamilies VI and VII are syntenic with mouse
401 subfamilies H and I on chromosome 13. Lemur subfamilies not sharing synteny with any mouse
402 subfamily include subfamilies II, VIII, and IX. The expanded subfamilies in Cheirogaleidae, IV,
403 VII, and IX, all map to different chromosomal regions of the *M. murinus* genome and were not
404 linked on an ancestral syntenic block based on comparisons between *M. murinus* and mouse.
405 Therefore subfamily expansions have occurred independently and not as tandem duplications of
406 a single genomic region.

407 Interestingly, when comparing all mammalian species examined, our results reveal that in
408 each species, one chromosome contains a very dense block of highly homologous subfamilies on
409 a backbone of mouse chromosome 7 synteny, referred to here as “V1R hotspots” (Figure 7B).
410 These hotspots usually contain receptors of the EF/III, D/IV, JK/V, and *Strep*/G subfamilies, and
411 cluster order is maintained with a few species-specific subfamily deletions. The chromosomal
412 synteny of the "hotspots" is rarely interrupted, and if interrupted, it is almost exclusively
413 interrupted by a stretch of synteny from another mouse chromosome containing V1Rs. These
414 interleaving regions in hotspots are usually chromosome 13 or 17, indicating that genomic

415 regions where V1Rs cluster are also subject to increased gene duplication rates. Interestingly, the
416 only putative intact members of the contracted human V1R repertoire are also contained within
417 this "hotspot" location and share homology with hotspot subfamilies.

418 Previous studies of Laurasiatheria have predicted that the V1R repertoires of cow, horse,
419 and dog consist mostly of highly orthologous loci with evolutionary conserved functions (Yohe
420 et al. 2018). While conserved function remains to be shown experimentally, retained synteny of
421 these Laurasiatherian V1Rs within hotspots across Mammalia supports the hypothesized ancient
422 origin of these subfamilies and reinforces the idea that V1Rs in these subfamilies are orthologous
423 in function (Ohara et al. 2009; Yohe et al. 2018). Mouse lemur V1Rs show striking structural
424 similarities to the functionally diverse repertoire of mouse and considering the independent gains
425 in copy number and novel subfamily evolution, coupled with variable rates of molecular
426 evolution and selective pressures, V1Rs in mouse lemurs may serve as an ideal system for
427 elucidating pheromone evolution in primates. Similar patterns of deep synteny have been
428 described for ~80 My of odorant receptor evolution in bees (Brand and Ramirez 2017).

429 Considered in this context, our results suggest that chemosensory gene family evolution may
430 follow similar molecular "rules" in organisms with vastly different natural histories, even when
431 evolved independently from different ancestral gene families, as would be the case comparing
432 mammals to insects.

433

434 **Conclusions**

435 We revealed that an expansion of the V1R gene family is shared across the dwarf and
436 mouse lemurs, and that duplicate V1R gene copies have been evolving under strong selective
437 pressures. Divergent patterns of molecular evolution among V1R subfamilies and diversity in

438 subfamily membership and abundance suggests that VIRs may serve as a test case for studying
439 the evolution of sensory drive in primates. Pheromone detection among nocturnal primates,
440 especially the morphologically cryptic mouse lemurs, may be more important for driving and
441 maintaining species boundaries than previously appreciated. Syntenic analyses with improved
442 genomic resources revealed strikingly similar genetic architecture between the expanded VIR
443 repertoires of mouse and mouse lemur, and that some VIR subfamilies have been maintained in
444 VIR “hotspots” across ~184 million years of mammalian evolution (dos Reis Mario et al. 2012).
445 Characterizing additional features of VIR hotspots across species will be important for future
446 studies translating experimental genetic studies in mice to primates such as mouse lemur.

447

448 **Materials and Methods**

449

450 **Sampling and DNA extraction**

451 To improve the resolution of the VIR repertoire expansion in lemurs, we sequenced the
452 genomes of *Microcebus griseorufus*, *M. mittermeieri*, *M. ravelobensis*, *M. tavaratra*, and *Mizra*
453 *zaza*. Tissue biopsies were taken from wild individuals in Madagascar from 1997-2015 and from
454 captive individuals at the Duke Lemur Center (Supplemental Table S13). To investigate within
455 species variation in VIR repertoires, we also resequenced eight individuals from the Duke
456 Lemur Center *Microcebus murinus* colony. Blood and tissue samples were collected in 2016 in
457 accordance with IACUC guidelines. For the novel strepsirrhine genomes, DNA was extracted
458 following manufacturer instructions using the Qiagen DNeasy Blood and Tissue kit, while DNA
459 from the *Microcebus murinus* resequenced individuals was extracted using the Qiagen
460 MagAttract Kit (Qiagen, Germantown, MD, USA).

461 **Genome Sequencing and Assembly**

462

463 The genomes of *Microcebus griseorufus*, *M. mittermeieri*, *M. tavaratra*, and *Mizra*
464 *zaza* were sequenced at the Baylor College of Medicine as approximately 400bp insert libraries
465 on a single lane of an Illumina HiSeq 3000 with paired-end 150bp reads. We sequenced
466 the *Microcebus ravelobensis* genome from two libraries, one with an average insert size of
467 570bp on an Illumina HiSeq 2000 at Florida State University and the other with a 500bp insert
468 library on 5.5% of both lanes of an Illumina NovaSeq at the Duke University GCB Sequencing
469 Core. We also generated two additional cheirogaleid assemblies for *Cheirogaleus sibreei* and *C.*
470 *medius* (Williams et al. 2019). *Cheirogaleus sibreei* was sequenced from a 300bp insert library
471 on the Illumina HiSeq 4000 at the Duke University GCB Sequencing Core with paired-end
472 150bp reads. A reference genome was generated and assembled for *Cheirogaleus medius* using
473 Dovetail Genomics. All other genomes were assembled using MaSuRCA v3.2.2 (Zimin et al.
474 2013). We assumed an insert size standard deviation of 15% and used automatic kmer selection.
475 However, we did not use MaSuRCA's scaffolds for annotation and downstream analyses.
476 Scaffolds were obtained from SSPACE (Boetzer et al. 2010), which also attempted to correct
477 assembly errors and extend contigs from MaSuRCA. *De novo* assembly statistics are available in
478 the supplementary material (Supplementary Table S1) as well as annotation details
479 (Supplementary Table S14) and SRA identifiers (Supplementary Table S15).

480 The eight *Microcebus murinus* individuals were resequenced from high molecular weight
481 DNA prepared using the 10X Genomics Chromium platform. Briefly, high-molecular weight
482 molecules of DNA are partitioned into gel beads with unique barcodes then prepared for Illumina
483 sequencing (Weisenfeld et al. 2017). The resulting short-read libraries are barcoded such that
484 individual "linked reads" can be traced back to their molecule of origin assisting the genomic

485 scaffolding process. The libraries were size selected to approximately 550bp and sequenced on
486 the Illumina HiSeq 4000 system at the Duke University GCB Sequencing Core. We then used
487 the 10X Genomics Supernova assembly software to *de novo* assemble the resequenced genomes
488 (version 2.0.1, 10x Genomics, San Francisco, CA, USA). One replicate individual was
489 sequenced twice, and genomes were assembled *de novo* from each individual library.

490 BUSCO version 3.0.2 and Assemblathon2 scripts were used to assess genome quality
491 statistics (Supplementary Figure S1; Supplementary Table S16; Simão et al. 2015). Additional
492 genomes analyzed in this study were downloaded from the NCBI genome database and include
493 all available Strepsirrhine genomes and additional high-quality primate and mammalian genomes
494 for phylogenetic coverage (Supplementary Table S16).

495

496 **V1R repertoire estimation and ancestral count reconstruction**

497 To assess total V1R repertoires in each species, tblastn searches (e-value cut-off = 0.001)
498 were conducted with the blast+ software suite (version ncbi-blast-2.6.0+; Altschul et al. 1990)
499 using available mouse and mouse lemur V1R query protein sequences downloaded from NCBI
500 GenBank against the genomes analyzed in this study (Camacho et al. 2009). Duplicate protein
501 sequences were removed from the query database using CD-HIT version 4.6 (Li and Godzik
502 2006). Bedtools merge (version 2.27.1) was used to merge overlapping hits within a genome, and
503 bedtools slop and getFasta were used to extract receptor candidate regions longer than 600bp
504 with 50 bp of upstream and downstream surrounding sequence (Quinlan and Hall 2010). For a
505 full list of V1R containing regions analyzed see Supplementary File X).

506 To remove potential pseudogenes from further analyses, we used Geneious version 9.0.5
507 to predict open reading frames (ORFs) and considered sequences intact if they contained an ORF

508 longer than 801bp. We then used MAFFT version 7.187 with the E-INS-i algorithm to align
509 intact sequences from all species using the iterative approach described in Yoder 2014 (Katoh
510 and Standley 2013; Yoder et al. 2014). The MAFFT algorithm is recommended for approaches
511 analyzing ancestral sequence reconstruction (Vialle et al. 2018). A gene phylogeny was
512 constructed using RAxML version 7.2.8 using the GTRGAMMAI nucleotide model with the
513 rapid bootstrapping and search for best ML scoring tree algorithm with 500 bootstraps
514 (Stamatakis 2014). We then assigned primate sequences to the subfamilies *Strep/I-IX* designated
515 in Hohenbrink 2012 (Hohenbrink et al. 2012). The number of intact V1Rs, percentage of intact
516 V1Rs, and the total V1R count were calculated for each species as well as subfamily
517 membership. We then used Count version 10.04 with the Wagner parsimony algorithm and a
518 gain penalty of 2 to infer total ancestral vomeronasal repertoire size and ancestral subfamily
519 membership (Csűrös and Miklos 2009; Csűrös 2010).

520

521 **Establishing synteny of V1Rs across mammalian species**

522 Genomes with chromosome level scaffolding information (*Mus musculus*, *Microcebus*
523 *murinus*, *Homo sapiens*, *Equus caballus*, *Bos taurus*, and *Canis familiaris*) were used to assess
524 chromosomal synteny of vomeronasal subfamilies among mammalian species. SynChro (Drillon
525 et al. 2014) version SynChro_osx (January 2015) was used to reconstruct synteny blocks
526 between each genome with *Mus musculus* as reference with a delta parameter of 2 using
527 GenBank annotation files from Ensembl release 93 (Figure 6; Supplemental Figures S8-S11;
528 Drillon et al. 2014). Orthologous block information was compared with vomeronasal receptor
529 location for each species (Figure 7A and B).

530

531 **Detecting evidence of positive selection**

532 Evidence for positive selection in V1R repertoires was evaluated with PAML 4.8e (Yang
533 2007). We used two different tests to detect both individual sites under pervasive positive
534 selection throughout the tree (sites models) and individual branches that show an episodic burst
535 of positive selection (branch-site models). For sites models, we applied two tests to each of the
536 nine subfamily trees and alignments: 1) Comparison of the null hypothesis that all sites are a
537 mixture of purifying and neutral rates of molecular evolution (M1a) and the alternative that
538 allows for a third class of sites under positive selection (M2a; Zhang et al. 2005). 2) A null
539 hypothesis that allows for a mixture of ten discretized beta-distributed site classes (M7), while
540 the alternative hypothesis allows an extra component under positive selection (M8; Yang et al.
541 2000). Each of the recognized lemur subfamilies were analyzed separately. The ggtree R
542 package (Yu et al. 2017) was used to extract subtrees for each subfamily and alignments were
543 parsed with Perl scripts. Because signatures of positive selection may be time-dependent
544 (Peterson and Masel 2009; Pegueroles et al. 2013), we explored variation in sites under positive
545 selection using six different taxonomic filters: 1) *Microcebus*, 2) Cheirogaleidae, 3)
546 Lemuriformes, 4) Strepsirrhini, 5) Primates, and 6) Euarchontoglires. For each site test, we
547 assumed the LRT was $\sim X^2_1$ and individual sites were detected using the Bayes empirical Bayes
548 procedure where the posterior probability of selection for each site was determined using the
549 MLE dN/dS for the positive selection rate class (Yang et al. 2005). Individual sites were
550 considered to have sufficient evidence for positive selection if the posterior probability was
551 greater than 0.95. Enrichment of sites under selection in transmembrane domains used simple
552 chi-square tests and Fisher exact tests in R (R Core Team 2018) for individual transmembrane
553 and loop domains. Transmembrane domains were predicted using *M. murinus* sequences from

554 subfamilies *Strep*/I through IX with TMHMM (Krogh et al. 2001) through the TMHMM server
555 (<http://www.cbs.dtu.dk/services/TMHMM/>; last accessed 29 January 2019). Since V1R genes
556 are expected to have seven transmembrane domains (Dulac and Axel 1995), only predicted
557 structures with seven transmembrane domains were used to determine transmembrane domain
558 boundaries in our alignment of the entire V1R repertoire. Predictions that had fewer or more than
559 seven transmembrane domains are assumed to be due to inaccuracies of TMHMM (Melén et al.
560 2003) and not real domain losses or gains.

561 Of important note, the entire V1R repertoire was prohibitively large for ML optimization
562 over the entire tree; we applied tests for selection to individual subfamilies to circumvent this
563 limitation. This strategy also provided a way to evaluate contributions of alignment and
564 topological errors to evidence of positive selection. First, we evaluated if the ML topology
565 estimated from the entire repertoire was a plausible hypothesis using AU tests (Shimodaira
566 2004). First, we estimated the ML topology and branch lengths for each subfamily using the
567 parsed alignments (i.e. the data was not re-aligned) using the same RAxML model and search
568 strategy as the first analysis. We then re-aligned translated amino acid data with MAFFT and
569 estimated phylogeny once more. Site log-likelihoods were then optimized for the three
570 topologies with RAxML and AU p-values computed with CONSEL using the default multiscale
571 bootstrapping strategy (Shimodaira and Hasegawa 2001). Bootstrap trees were also collected for
572 the re-aligned data, but bipartitions were drawn onto the topologies parsed from the entire V1R
573 repertoire tree. The ratio of bootstrap support values was used to identify potential topological
574 errors; bipartitions in the original topology that are absent when the sequences for each
575 subfamily were re-aligned. Site tests were run for both the parsed and re-aligned data to check
576 for consistency in the inference of sites under positive selection across alignments.

577 Branch-site tests (Zhang et al. 2005) were performed for each branch for each subfamily,
578 except subfamily III, which was still computationally limiting. Each test assumed the LRT was
579 $\sim X^2_1$, but we applied the Benjamini-Hochberg multiple testing correction (Benjamini and
580 Hochberg 1995). With this correction, we do expect some false positives, but the family-wise
581 error rate should be below 5% (Anisimova and Yang 2007) while not underpowering tests
582 towards the tips of the trees (dos Reis and Yang 2011). Tests were only performed on the parsed
583 topology without removing any species, but branches with evidence of episodic positive
584 selection and the bootstrap ratios with re-aligned data were mapped to nodes of the subtree
585 topologies using ggtree to help identify cases where topological errors might lead to false
586 signatures of positive selection (Mendes and Hahn 2016). Individual sites with evidence of
587 episodic positive selection were evaluated using the Bayes empirical Bayes procedure (Yang et
588 al. 2005).

589 **Data Access**

590 Newly sequenced genome data will be made available through NCBI upon publication.
591 Complete record information is given in Supplementary Material (Supplementary Table S15).

592

593 **Acknowledgements**

594 We thank the Malagasy authorities for permission to conduct this research and Duke Lemur
595 Center staff, especially Erin Ehmke, Bobby Schopler, and Cathy Williams, for providing the
596 *Microcebus murinus* and *Mirza zaza* tissue samples. We are grateful to our colleagues at Baylor
597 College of Medicine, Jeff Rogers and Kim Worley, for many insightful discussions of mouse
598 lemur genomics. Phillip Brand and Jeff Thorne provided critical review of the manuscript
599 leading to its significant improvement. We thank Simon Gregory's lab for preparing the 10x

600 Genomics libraries. We are grateful for the support of Duke Research Computing and the Duke
601 Data Commons (NIH 1S10OD018164-01) and appreciate the donation of free sequencing for
602 *Microcebus ravelobensis* provided by the Duke GCB Sequencing Core. ADY gratefully
603 acknowledges support from the John Simon Guggenheim Foundation and the Alexander von
604 Humboldt Foundation during the writing phase of this project. The study was funded by a
605 National Science Foundation Grant DEB-1354610 to ADY and DWW and Duke University
606 startup funds to ADY. This is Duke Lemur Center publication no. XXX.

607

608

609

610

611

612

613 **References**

- 614 Adipietro KA, Matsunami H, Zhuang H. 2012. Functional Evolution of Primate Odorant
615 Receptors. In: Hirai H, Imai H, Go Y, editors. *Post-Genome Biology of Primates*. Tokyo:
616 Springer Tokyo. p. 63–78. Available from:
617 http://www.springerlink.com/index/10.1007/978-4-431-54011-3_5
- 618 Altschul SF, Gish W, Miller W, Myers EW, Lipman DJ. 1990. Basic local alignment search tool.
619 *Journal of Molecular Biology* 215:403–410.
- 620 Anisimova M, Yang Z. 2007. Multiple Hypothesis Testing to Detect Lineages under Positive
621 Selection that Affects Only a Few Sites. *Molecular Biology and Evolution* 24:1219–
622 1228.
- 623 Bear DM, Lassance J-M, Hoekstra HE, Datta SR. 2016. The Evolving Neural and Genetic
624 Architecture of Vertebrate Olfaction. *Current Biology* 26:R1039–R1049.
- 625 Benjamini Y, Hochberg Y. 1995. Controlling the False Discovery Rate: A Practical and
626 Powerful Approach to Multiple Testing. *Journal of the Royal Statistical Society: Series B*
627 (Methodological) 57:289–300.
- 628 Boetzer M, Henkel CV, Jansen HJ, Butler D, Pirovano W. 2010. Scaffolding pre-assembled
629 contigs using SSPACE. *Bioinformatics* 27:578–579.
- 630 Boillat M, Challet L, Rossier D, Kan C, Carleton A, Rodriguez I. 2015. The Vomeronasal
631 System Mediates Sick Conspecific Avoidance. *Current Biology* 25:251–255.
- 632 Borges R, Johnson WE, O’Brien SJ, Gomes C, Heesy CP, Antunes A. 2018. Adaptive genomic
633 evolution of opsins reveals that early mammals flourished in nocturnal environments.
634 *BMC Genomics* [Internet] 19. Available from:
635 <https://bmcgenomics.biomedcentral.com/articles/10.1186/s12864-017-4417-8>
- 636 Boschat C, Pelofi C, Randin O, Roppolo D, Luscher C, Broillet M-C, Rodriguez I. 2002.
637 Pheromone detection mediated by a V1r vomeronasal receptor. *Nat Neurosci* 5:1261–
638 1262.
- 639 Boughman JW. 2002. How sensory drive can promote speciation. *Trends in Ecology &*
640 *Evolution* 17:571–577.
- 641 Brand P, Hinojosa-Díaz IA, Ayala R, Daigle M, Yurrita Obiols CL, Eltz T, Ramírez SR. 2019.
642 An olfactory receptor gene underlies reproductive isolation in perfume-collecting orchid
643 bees. *bioRxiv*:537423.
- 644 Brand P, Ramírez SR. 2017. The Evolutionary Dynamics of the Odorant Receptor Gene Family
645 in Corbiculate Bees. *Genome Biology and Evolution* 9: 2023-2036.
- 646 Camacho C, Coulouris G, Avagyan V, Ma N, Papadopoulos J, Bealer K, Madden TL. 2009.
647 BLAST+: architecture and applications. *BMC Bioinformatics* 10:421.

- 648 Chen F-C, Chen C-J, Chuang T-J, Li W-H. 2010. Gene Family Size Conservation Is a Good
649 Indicator of Evolutionary Rates. *Molecular Biology and Evolution* 27:1750–1758.
- 650 Chung AG, Belone PM, Bímová BV, Karn RC, Laukaitis CM. 2017. Studies of an *Androgen-*
651 *Binding Protein* Knockout Corroborate a Role for Salivary ABP in Mouse
652 Communication. *Genetics* 205:1517–1527.
- 653 Csűrös M. 2010. Count: evolutionary analysis of phylogenetic profiles with parsimony and
654 likelihood. *Bioinformatics* 26:1910–1912.
- 655 Csűrös M, Miklos I. 2009. Streamlining and Large Ancestral Genomes in Archaea Inferred with
656 a Phylogenetic Birth-and-Death Model. *Molecular Biology and Evolution* 26:2087–2095.
- 657 Dai Z, Xiong Y, Dai X. 2014. Neighboring Genes Show Interchromosomal Colocalization after
658 Their Separation. *Mol Biol Evol* 31:1166–1172.
- 659 Del Punta K, Leinders-Zufall T, Rodriguez I, Jukam D, Wysocki CJ, Ogawa S, Zufall F,
660 Mombaerts P. 2002. Deficient pheromone responses in mice lacking a cluster of
661 vomeronasal receptor genes. *Nature* 419:70–74.
- 662 Des Marais DL, Rausher MD. 2008. Escape from adaptive conflict after duplication in an
663 anthocyanin pathway gene. *Nature* 454:762–765.
- 664 Dinka H, Le MT. 2017. Analysis of Pig Vomeronasal Receptor Type 1 (V1R) Promoter Region
665 Reveals a Common Promoter Motif but Poor CpG Islands. *Animal Biotechnology*:1–8.
- 666 Dopman EB, Robbins PS, Seaman A. 2010. COMPONENTS OF REPRODUCTIVE
667 ISOLATION BETWEEN NORTH AMERICAN PHEROMONE STRAINS OF THE
668 EUROPEAN CORN BORER. *Evolution* 64:881–902.
- 669 dos Reis Mario, Inoue Jun, Hasegawa Masami, Asher Robert J., Donoghue Philip C. J., Yang
670 Ziheng. 2012. Phylogenomic datasets provide both precision and accuracy in estimating
671 the timescale of placental mammal phylogeny. *Proceedings of the Royal Society B:*
672 *Biological Sciences* 279:3491–3500.
- 673 Drea CM. 2015. D'scent of man: A comparative survey of primate chemosignaling in relation to
674 sex. *Hormones and Behavior* 68:117–133.
- 675 Drillon G, Carbone A, Fischer G. 2014. SynChro: A Fast and Easy Tool to Reconstruct and
676 Visualize Synteny Blocks along Eukaryotic Chromosomes. Fairhead C, editor. *PLoS ONE*
677 9:e92621.
- 678 Dulac C, Axel R. 1995. A novel family of genes encoding putative pheromone receptors in
679 mammals. *Cell* 83:195–206.
- 680 Fu X, Yan Y, Xu PS, Geerlof-Vidavsky I, Chong W, Gross ML, Holy TE. 2015. A Molecular
681 Code for Identity in the Vomeronasal System. *Cell* 163:313–323.

- 682 Guschanski K, Warnefors M, Kaessmann H. 2017. The evolution of duplicate gene expression in
683 mammalian organs. *Genome Research* [Internet]. Available from:
684 <http://genome.cshlp.org/content/early/2017/08/04/gr.215566.116.abstract>
- 685 Haga-Yamanaka S, Ma L, He J, Qiu Q, Lavis LD, Looger LL, Yu CR. 2014. Integrated action of
686 pheromone signals in promoting courtship behavior in male mice. *Elife* 3:e03025.
- 687 Hawkins MTR, Culligan RR, Frasier CL, Dikow RB, Hagensohn R, Lei R, Louis EE. 2018.
688 Genome sequence and population declines in the critically endangered greater bamboo
689 lemur (*Prolemur simus*) and implications for conservation. *BMC Genomics* [Internet] 19.
690 Available from: [https://bmcgenomics.biomedcentral.com/articles/10.1186/s12864-018-](https://bmcgenomics.biomedcentral.com/articles/10.1186/s12864-018-4841-4)
691 [4841-4](https://bmcgenomics.biomedcentral.com/articles/10.1186/s12864-018-4841-4)
- 692 Hohenbrink P, Dempewolf S, Zimmermann E, Mundy NI, Radespiel U. 2014. Functional
693 promiscuity in a mammalian chemosensory system: extensive expression of vomeronasal
694 receptors in the main olfactory epithelium of mouse lemurs. *Frontiers in Neuroanatomy*
695 [Internet] 8. Available from:
696 <http://journal.frontiersin.org/article/10.3389/fnana.2014.00102/abstract>
- 697 Hohenbrink P, Radespiel U, Mundy NI. 2012. Pervasive and Ongoing Positive Selection in the
698 Vomeronasal-1 Receptor (V1R) Repertoire of Mouse Lemurs. *Molecular Biology and*
699 *Evolution* 29:3807–3816.
- 700 Hotaling S, Foley ME, Lawrence NM, Bocanegra J, Blanco MB, Rasoloarison R, Kappeler PM,
701 Barrett MA, Yoder AD, Weisrock DW. 2016. Species discovery and validation in a
702 cryptic radiation of endangered primates: coalescent-based species delimitation in
703 Madagascar’s mouse lemurs. *Molecular Ecology* 25:2029–2045.
- 704 Hughes GM, Boston ESM, Finarelli JA, Murphy WJ, Higgins DG, Teeling EC. 2018. The Birth
705 and Death of Olfactory Receptor Gene Families in Mammalian Niche Adaptation. Satta
706 Y, editor. *Molecular Biology and Evolution* 35:1390–1406.
- 707 Hurst JL, Beynon RJ, Armstrong SD, Davidson AJ, Roberts SA, Gómez-Baena G, Smadja CM,
708 Ganem G. 2017. Molecular heterogeneity in major urinary proteins of *Mus musculus*
709 subspecies: potential candidates involved in speciation. *Scientific Reports* [Internet] 7.
710 Available from: <http://www.nature.com/articles/srep44992>
- 711 Isogai Y, Si S, Pont-Lezica L, Tan T, Kapoor V, Murthy VN, Dulac C. 2011. Molecular
712 organization of vomeronasal chemoreception. *Nature* 478:241–245.
- 713 Kambere MB, Lane RP. 2007. Co-regulation of a large and rapidly evolving repertoire of
714 odorant receptor genes. *BMC Neuroscience* 8:S2.
- 715 Kambere MB, Lane RP. 2009. Exceptional LINE Density at V1R Loci: The Lyon Repeat
716 Hypothesis Revisited on Autosomes. *Journal of Molecular Evolution* 68:145–159.

- 717 Karn RC, Young JM, Laukaitis CM. 2010. A Candidate Subspecies Discrimination System
718 Involving a Vomeronasal Receptor Gene with Different Alleles Fixed in *M. m.*
719 *domesticus* and *M. m. musculus*. PLoS ONE 5:e12638.
- 720 Katoh K, Standley DM. 2013. MAFFT Multiple Sequence Alignment Software Version 7:
721 Improvements in Performance and Usability. Mol Biol Evol 30:772–780.
- 722 Keller TE, Yi SV. 2014. DNA methylation and evolution of duplicate genes. Proc Natl Acad Sci
723 USA 111:5932.
- 724 Kobilka BK, Kobilka TS, Daniel K, Regan JW, Caron MG, Lefkowitz RJ. 1988. Chimeric alpha
725 2-,beta 2-adrenergic receptors: delineation of domains involved in effector coupling and
726 ligand binding specificity. Science 240:1310–1316.
- 727 Krogh A, Larsson B, von Heijne G, Sonnhammer ELL. 2001. Predicting transmembrane protein
728 topology with a hidden markov model: application to complete genomes 11 Edited by F.
729 Cohen. Journal of Molecular Biology 305:567–580.
- 730 Kurzweil VC, Getman M, Comparative Sequencing Program N, Green ED, Lane RP. 2009.
731 Dynamic evolution of V1R putative pheromone receptors between *Mus musculus* and
732 *Mus spretus*. BMC Genomics 10:74.
- 733 Lane RP, Cutforth T, Axel R, Hood L, Trask BJ. 2002. Sequence analysis of mouse vomeronasal
734 receptor gene clusters reveals common promoter motifs and a history of recent
735 expansion. Proceedings of the National Academy of Sciences 99:291–296.
- 736 Larsen PA, Harris RA, Liu Y, Murali SC, Campbell CR, Brown AD, Sullivan BA, Shelton J,
737 Brown SJ, Raveendran M, et al. 2017. Hybrid de novo genome assembly and centromere
738 characterization of the gray mouse lemur (*Microcebus murinus*). BMC Biology [Internet]
739 15. Available from: [https://bmcbiol.biomedcentral.com/articles/10.1186/s12915-017-](https://bmcbiol.biomedcentral.com/articles/10.1186/s12915-017-0439-6)
740 0439-6
- 741 Larsen PA, Heilman AM, Yoder AD. 2014. The utility of PacBio circular consensus sequencing
742 for characterizing complex gene families in non-model organisms. BMC Genomics
743 15:720.
- 744 Lei R, Frasier CL, McLain AT, Taylor JM, Bailey CA, Engberg SE, Ginter AL,
745 Randriamampionona R, Groves CP, Mittermeier RA, et al. 2014. Revision of
746 Madagascar's Dwarf Lemurs (*Cheirogaleidae: Cheirogaleus*): Designation of Species,
747 Candidate Species Status and Geographic Boundaries Based on Molecular and
748 Morphological Data. Primate Conservation 28:9–35.
- 749 Leinders-Zufall T, Lane AP, Puche AC, Ma W, Novotny MV, Shipley MT, Zufall F. 2000.
750 Ultrasensitive pheromone detection by mammalian vomeronasal neurons. Nature
751 405:792–796.
- 752 Li W, Godzik A. 2006. Cd-hit: a fast program for clustering and comparing large sets of protein
753 or nucleotide sequences. Bioinformatics 22:1658–1659.

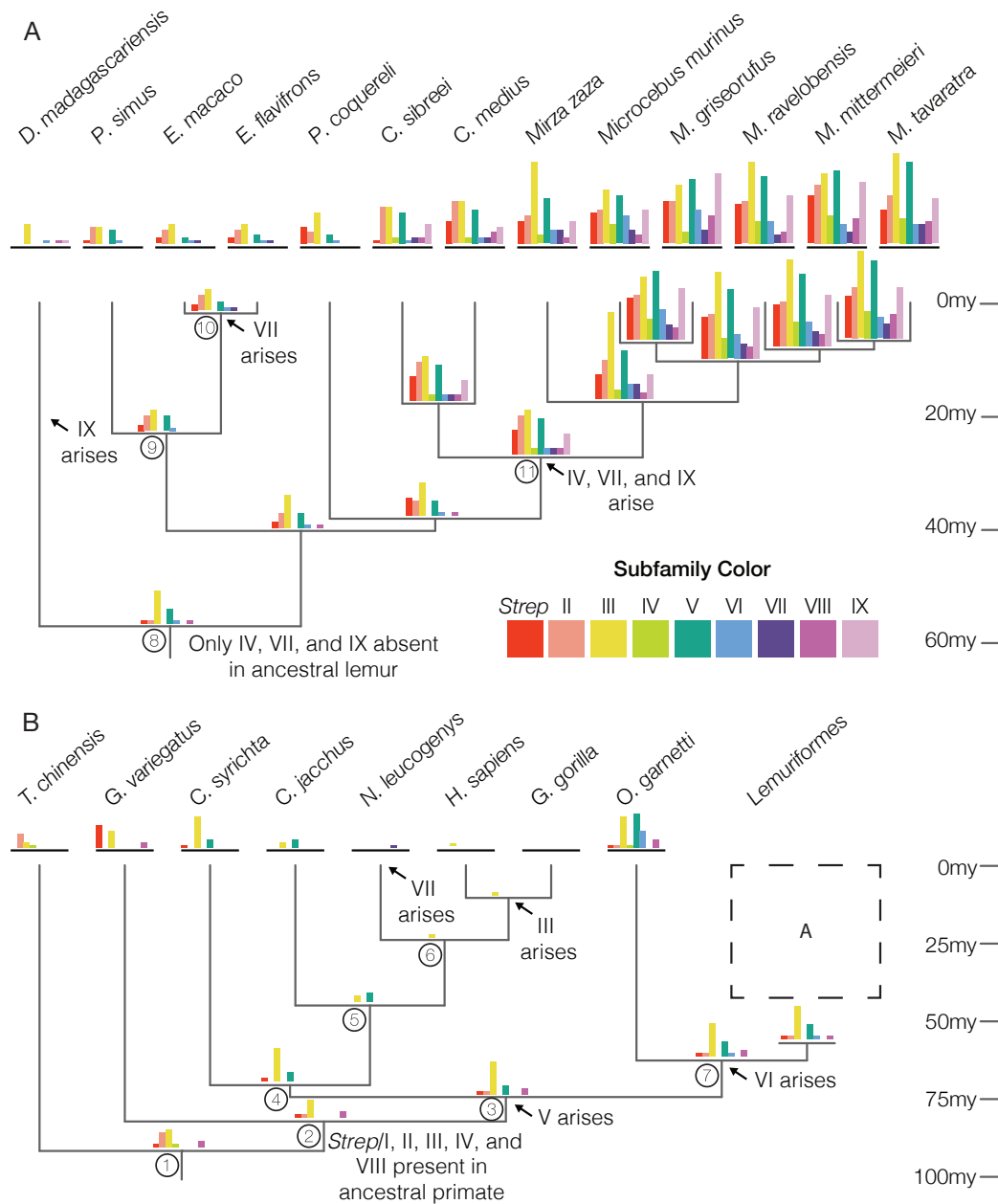
- 754 Loire E, Tusso S, Caminade P, Severac D, Boursot P, Ganem G, Smadja CM. 2017. Do changes
755 in gene expression contribute to sexual isolation and reinforcement in the house mouse?
756 *Molecular Ecology* 26:5189–5202.
- 757 Luo M, Fee MS, Katz LC. 2003. Encoding Pheromonal Signals in the Accessory Olfactory Bulb
758 of Behaving Mice. *Science* 299:1196–1201.
- 759 Lynch M, Conery JS. 2000. The Evolutionary Fate and Consequences of Duplicate Genes.
760 *Science* 290:1151–1155.
- 761 Makova KD, Li W-H. 2003. Divergence in the Spatial Pattern of Gene Expression Between
762 Human Duplicate Genes. *Genome Res.* 13:1638–1645.
- 763 Melén K, Krogh A, von Heijne G. 2003. Reliability measures for membrane protein topology
764 prediction algorithms. *J Mol Biol.* 327:735–744.
765
- 766 Mendelson TC. 2003. Evidence of Intermediate and Asymmetrical Behavioral Isolation Between
767 Orangethroat and Orangebelly darters (Teleostei:Percidae). *The American Midland*
768 *Naturalist* 150:343–348.
- 769 Mendes FK, Hahn MW. 2016. Gene Tree Discordance Causes Apparent Substitution Rate
770 Variation. *Systematic Biology* 65:711–721.
- 771 Meyer WK, Venkat A, Kermany AR, van de Geijn B, Zhang S, Przeworski M. 2015.
772 Evolutionary history inferred from the de novo assembly of a nonmodel organism, the
773 blue-eyed black lemur. *Molecular Ecology* 24:4392–4405.
- 774 Michaloski JS, Galante PAF, Nagai MH, Armelin-Correa L, Chien M-S, Matsunami H, Malnic
775 B. 2011. Common Promoter Elements in Odorant and Vomeronasal Receptor
776 Genes. Meyerhof W, editor. *PLoS ONE* 6:e29065.
- 777 Moriya-Ito K, Hayakawa T, Suzuki H, Hagino-Yamagishi K, Nikaido M. 2018. Evolution of
778 vomeronasal receptor 1 (V1R) genes in the common marmoset (*Callithrix jacchus*).
779 *Gene* 642:343–353.
- 780 Nei M, Gu X, Sitnikova T. 1997. Evolution by the birth-and-death process in multigene families
781 of the vertebrate immune system. *Proc Natl Acad Sci USA* 94:7799.
- 782 Nikaido M, Ota T, Hirata T, Suzuki H, Satta Y, Aibara M, Mzighani SI, Sturmbauer C, Hagino-
783 Yamagishi K, Okada N. 2014. Multiple Episodic Evolution Events in V1R Receptor
784 Genes of East-African Cichlids. *Genome Biol Evol* 6:1135–1144.
- 785 Nozawa M, Kawahara Y, Nei M. 2007. Genomic drift and copy number variation of sensory
786 receptor genes in humans. *Proc Natl Acad Sci USA* 104:20421.
- 787 Ohara H, Nikaido M, Date-Ito A, Mogi K, Okamura H, Okada N, Takeuchi Y, Mori Y, Hagino-
788 Yamagishi K. 2009. Conserved repertoire of orthologous vomeronasal type 1 receptor
789 genes in ruminant species. *BMC Evolutionary Biology* 9:233.

- 790 O'Toole ÁN, Hurst LD, McLysaght A. 2018. Faster Evolving Primate Genes Are More Likely to
791 Duplicate. *Mol Biol Evol* 35:107–118.
- 792 Palczewski K, Kumasaka T, Hori T, Behnke CA, Motoshima H, Fox BA, Trong IL, Teller DC,
793 Okada T, Stenkamp RE, et al. 2000. Crystal Structure of Rhodopsin: A G Protein-
794 Coupled Receptor. *Science* 289:739–745.
- 795 Papes F, Logan DW, Stowers L. 2010. The Vomeronasal Organ Mediates Interspecies Defensive
796 Behaviors through Detection of Protein Pheromone Homologs. *Cell* 141:692–703.
- 797 Park SH, Podlaha O, Grus WE, Zhang J. 2011. The Microevolution of V1r Vomeronasal
798 Receptor Genes in Mice. *Genome Biology and Evolution* 3:401–412.
- 799 Pegueroles C, Laurie S, Albà MM. 2013. Accelerated Evolution after Gene Duplication: A
800 Time-Dependent Process Affecting Just One Copy. *Molecular Biology and Evolution*
801 30:1830–1842.
- 802 Perret M. 1996. Manipulation of sex ratio at birth by urinary cues in a prosimian primate.
803 *Behavioral Ecology and Sociobiology* 38:259–266.
- 804 Perret M, Colas S. 1997. Manipulation of sex ratio at birth and maternal investment in female
805 mouse lemurs (*Microcebus murinus*, Primates). *Applied Animal Behaviour Science*
806 51:275–283.
- 807 Perry GH, Reeves D, Melsted P, Ratan A, Miller W, Michelini K, Louis EE, Pritchard JK,
808 Mason CE, Gilad Y. 2012. A Genome Sequence Resource for the Aye-Aye (*Daubentonia*
809 *madagascariensis*), a Nocturnal Lemur from Madagascar. *Genome Biology and Evolution*
810 4:126–135.
- 811 Peterson GI, Masel J. 2009. Quantitative Prediction of Molecular Clock and Ka/Ks at Short
812 Timescales. *Molecular Biology and Evolution* 26:2595–2603.
- 813 Pilpel Y, Lancet D. 1999. The variable and conserved interfaces of modeled olfactory receptor
814 proteins. *Protein Science* 8:969–977.
- 815 Quinlan AR, Hall IM. 2010. BEDTools: a flexible suite of utilities for comparing genomic
816 features. *Bioinformatics* 26:841–842.
- 817 dos Reis M, Gunnell GF, Barba-Montoya J, Wilkins A, Yang Z, Yoder AD. 2018. Using
818 Phylogenomic Data to Explore the Effects of Relaxed Clocks and Calibration Strategies
819 on Divergence Time Estimation: Primates as a Test Case. Ho S, editor. *Systematic*
820 *Biology* 67:594–615.
- 821 dos Reis M, Yang Z. 2011. Approximate Likelihood Calculation on a Phylogeny for Bayesian
822 Estimation of Divergence Times. *Molecular Biology and Evolution* 28:2161–2172.

- 823 Schmitz J, Noll A, Raabe CA, Churakov G, Voss R, Kiefmann M, Rozhdestvensky T, Brosius J,
824 Baertsch R, Clawson H, et al. 2016. Genome sequence of the basal haplorrhine primate
825 *Tarsius syrichta* reveals unusual insertions. *Nature Communications* 7:12997.
- 826 Servedio MR, Boughman JW. 2017. The Role of Sexual Selection in Local Adaptation and
827 Speciation. *Annual Review of Ecology, Evolution, and Systematics* 48:85–109.
- 828 Servedio MR, Noor MAF. 2003. The Role of Reinforcement in Speciation: Theory and Data.
829 *Annu. Rev. Ecol. Evol. Syst.* 34:339–364.
- 830 Shimodaira H. 2004. Approximately unbiased tests of regions using multistep-multiscale
831 bootstrap resampling. *The Annals of Statistics* 32:2616–2641.
- 832 Shimodaira H, Hasegawa M. 2001. CONSEL: for assessing the confidence of phylogenetic tree
833 selection. *Bioinformatics* 17:1246–1247.
- 834 Simão FA, Waterhouse RM, Ioannidis P, Kriventseva EV, Zdobnov EM. 2015. BUSCO:
835 assessing genome assembly and annotation completeness with single-copy orthologs.
836 *Bioinformatics* 31:3210–3212.
- 837 Smadja CM, Loire E, Caminade P, Thoma M, Latour Y, Roux C, Thoss M, Penn DJ, Ganem G,
838 Boursot P. 2015. Seeking signatures of reinforcement at the genetic level: a hitchhiking
839 mapping and candidate gene approach in the house mouse. *Molecular Ecology* 24:4222–
840 4237.
- 841 Stamatakis A. 2014. RAxML version 8: a tool for phylogenetic analysis and post-analysis of
842 large phylogenies. *Bioinformatics* 30:1312–1313.
- 843 Sterling EJ, Richard AF. 1995. Social Organization in the Aye-Aye (*Daubentonia*
844 *Madagascariensis*) and the Perceived Distinctiveness of Nocturnal Primates. In: Alterman
845 L, Doyle GA, Izard MK, editors. *Creatures of the Dark: The Nocturnal Prosimians*.
846 Boston, MA: Springer US. p. 439–451. Available from: https://doi.org/10.1007/978-1-4757-2405-9_26
847
- 848 Stewart R, Lane RP. 2007. V1R promoters are well conserved and exhibit common putative
849 regulatory motifs. *BMC Genomics* 8:253.
- 850 Sündermann D, Scheumann M, Zimmermann E. 2008. Olfactory predator recognition in
851 predator-naïve gray mouse lemurs (*Microcebus murinus*). *Journal of Comparative*
852 *Psychology* 122:146–155.
- 853 Tan Y, Yoder AD, Yamashita N, Li W-H. 2005. Evidence from opsin genes rejects nocturnality
854 in ancestral primates. *Proceedings of the National Academy of Sciences* 102:14712–
855 14716.
- 856 Vialle RA, Tamuri AU, Goldman N. 2018. Alignment Modulates Ancestral Sequence
857 Reconstruction Accuracy. Thorne J, editor. *Molecular Biology and Evolution* 35:1783–
858 1797.

- 859 Wang G, Shi P, Zhu Z, Zhang Y -p. 2010. More Functional V1R Genes Occur in Nest-Living
860 and Nocturnal Terricolous Mammals. *Genome Biology and Evolution* 2:277–283.
- 861 Weisenfeld NI, Kumar V, Shah P, Church DM, Jaffe DB. 2017. Direct determination of diploid
862 genome sequences. *Genome Res.* [Internet]. Available from:
863 <http://genome.cshlp.org/content/early/2017/03/15/gr.214874.116>
- 864 Williams RC, Blanco MB, Poelstra JW, Hunnicutt KE, Comeault AA, Yoder AD. 2019.
865 Conservation genomic analysis reveals ancient introgression and declining levels of
866 genetic diversity in Madagascar's hibernating dwarf lemurs. bioRxiv doi:
867 <https://doi.org/10.1101/620724>
868
- 869 Xie T, Yang Q-Y, Wang X-T, McLysaght A, Zhang H-Y. 2016. Spatial Colocalization of
870 Human Ohnolog Pairs Acts to Maintain Dosage-Balance. *Mol Biol Evol* 33:2368–2375.
- 871 Yang L, Gaut BS. 2011. Factors that Contribute to Variation in Evolutionary Rate among
872 Arabidopsis Genes. *Mol Biol Evol* 28:2359–2369.
- 873 Yang Z. 2007. PAML 4: Phylogenetic Analysis by Maximum Likelihood. *Molecular Biology*
874 *and Evolution* 24:1586–1591.
- 875 Yang Z, Nielsen R, Goldman N, Pedersen A-MK. 2000. Codon-Substitution Models for
876 Heterogeneous Selection Pressure at Amino Acid Sites. *Genetics* 155:431.
- 877 Yang Z, Wong WSW, Nielsen R. 2005. Bayes Empirical Bayes Inference of Amino Acid Sites
878 Under Positive Selection. *Molecular Biology and Evolution* 22:1107–1118.
- 879 Yang Z, Yoder AD. 2003. Comparison of Likelihood and Bayesian Methods for Estimating
880 Divergence Times Using Multiple Gene Loci and Calibration Points, with Application to
881 a Radiation of Cute-Looking Mouse Lemur Species. *Systematic Biology* 52:705–716.
- 882 Yoder AD, Chan LM, dos Reis M, Larsen PA, Campbell CR, Rasoloarison R, Barrett M, Roos
883 C, Kappeler P, Bielski J, et al. 2014. Molecular Evolutionary Characterization of a
884 V1R Subfamily Unique to Strepsirrhine Primates. *Genome Biology and Evolution* 6:213–
885 227.
- 886 Yoder AD, Larsen PA. 2014. The molecular evolutionary dynamics of the vomeronasal receptor
887 (class 1) genes in primates: a gene family on the verge of a functional breakdown.
888 *Frontiers in Neuroanatomy* [Internet] 8. Available from:
889 <http://journal.frontiersin.org/article/10.3389/fnana.2014.00153/abstract>
- 890 Yoder AD, Weisrock DW, Rasoloarison RM, Kappeler PM. 2016. Cheirogaleid diversity and
891 evolution: big questions about small primates. In: Lehman SM, Radespiel U,
892 Zimmermann E, editors. *The Dwarf and Mouse Lemurs of Madagascar*. Cambridge:
893 Cambridge University Press. p. 3–20. Available from:
894 <https://www.cambridge.org/core/product/identifier/CBO9781139871822A010/type/book>
895 _part

- 896 Yohe LR, Brand P. 2018. Evolutionary ecology of chemosensation and its role in sensory
897 drive. Fuller R, editor. *Current Zoology* 64:525–533.
- 898 Yohe LR, Davies KT, Rossiter SJ, Davalos L. 2018. Expressed vomeronasal type-1 receptors
899 (V1rs) in bats uncover conserved mechanisms of social chemical signaling. bioRxiv
900 [Internet]. Available from: <http://biorxiv.org/content/early/2018/04/05/293472.abstract>
- 901 Young JM, Massa HF, Hsu L, Trask BJ. 2010. Extreme variability among mammalian V1R gene
902 families. *Genome Research* 20:10–18.
- 903 Yu G, Smith DK, Zhu H, Guan Y, Lam TT-Y. 2017. ggtree: an r package for visualization and
904 annotation of phylogenetic trees with their covariates and other associated data. *Methods*
905 *in Ecology and Evolution* 8:28–36.
- 906 Zhang J, Nielsen R, Yang Z. 2005. Evaluation of an Improved Branch-Site Likelihood Method
907 for Detecting Positive Selection at the Molecular Level. *Molecular Biology and*
908 *Evolution* 22:2472–2479.
- 909 Zhang J, Rosenberg HF, Nei M. 1998. Positive Darwinian selection after gene duplication in
910 primate ribonuclease genes. *Proc Natl Acad Sci USA* 95:3708.
- 911 Zimin AV, Marçais G, Puiu D, Roberts M, Salzberg SL, Yorke JA. 2013. The MaSuRCA
912 genome assembler. *Bioinformatics* 29:2669–2677.
- 913
- 914

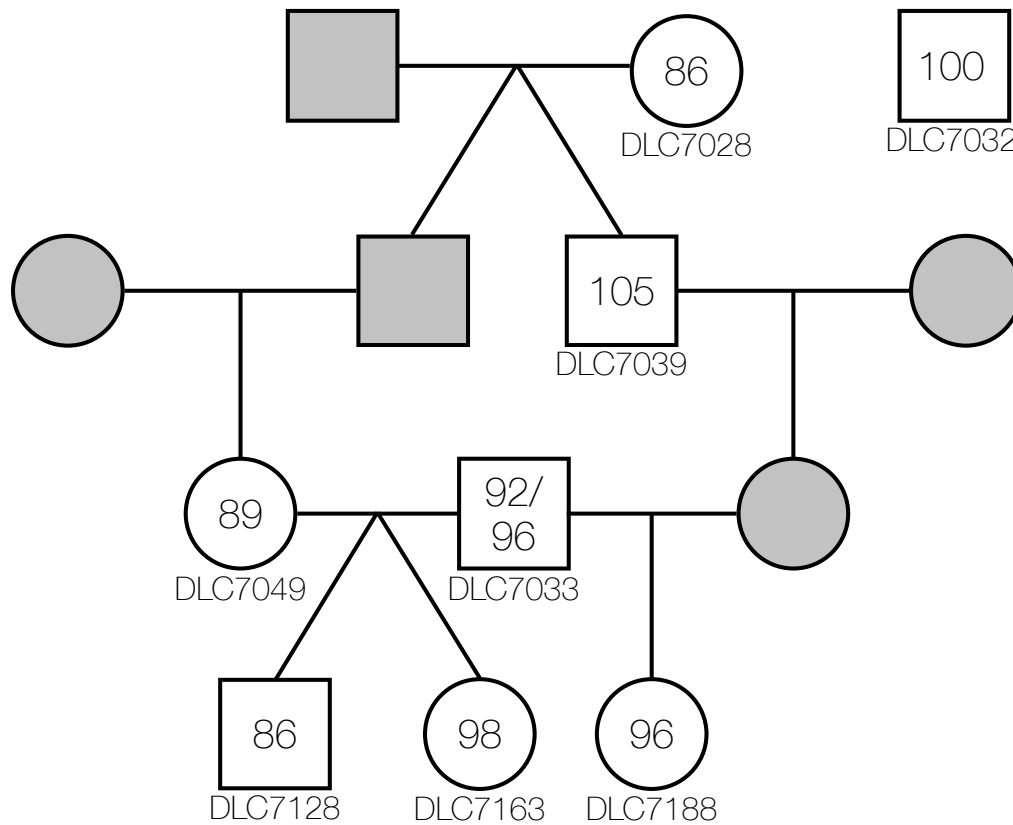


915

916

917 **Figure 1. V1R subfamily membership across the primate phylogeny.** Membership was
 918 assessed for available strepsirrhine genomes (A) and for select primate outgroups (B) and
 919 estimated using the Count software for ancestral lineages. Bar graphs show absolute gene count
 920 for each subfamily. Predicted gene subfamily origins are annotated with arrows. Tree adapted
 921 from dos Reis 2018 (dos Reis et al. 2018). Circled node numbers correspond with Table 1.

922



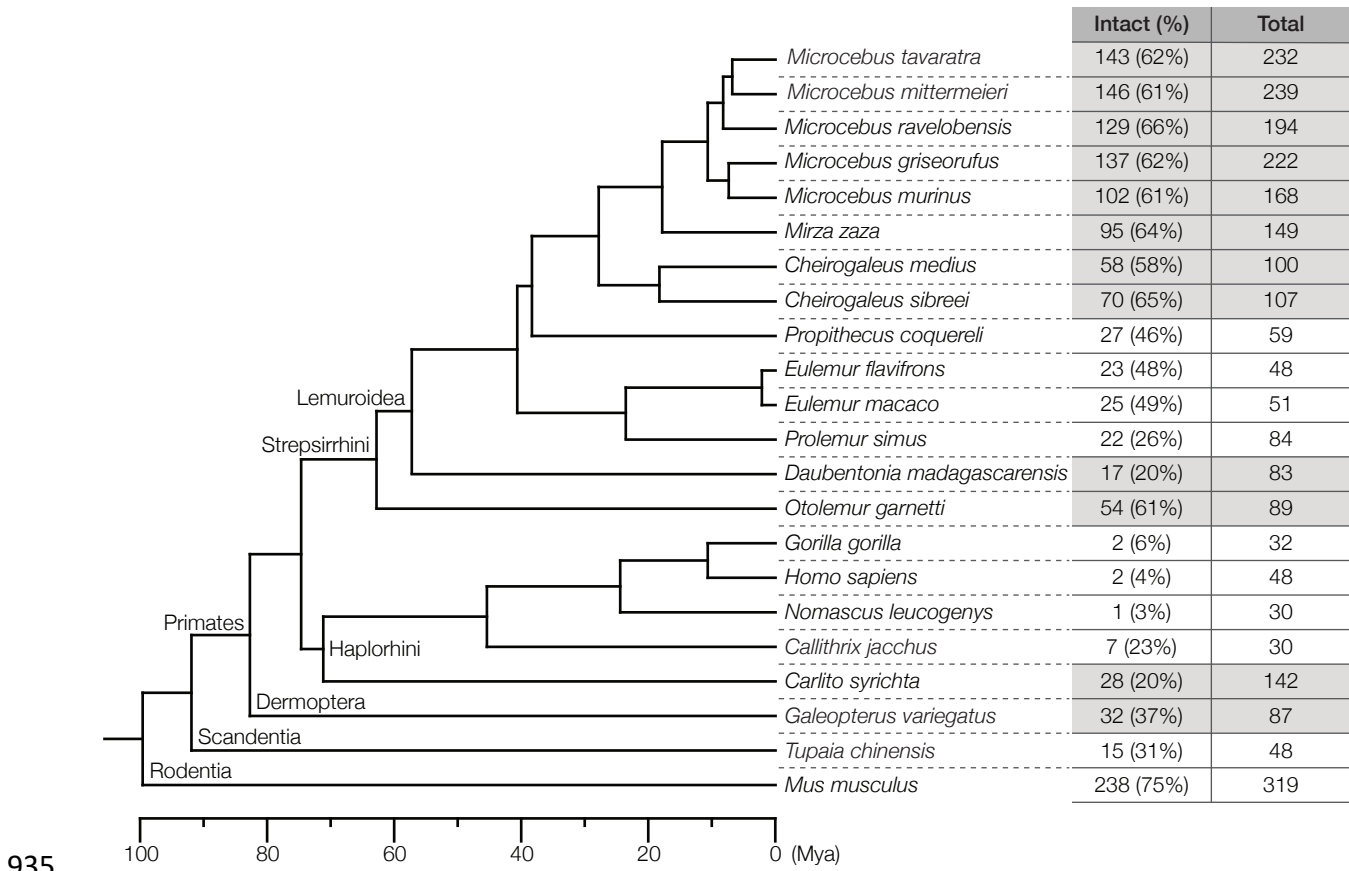
923

924

925 **Figure 2. Intraspecific variation in V1R repertoire size estimates across eight closely-**
926 **related *Microcebus murinus* individuals.** Genomes were *de novo* assembled and mined for loci
927 with significant V1R homology and an ORF longer than 801bp. Individual DLC7033 was
928 sequenced twice and repertoire size estimates are reported for both assemblies. Squares
929 represent males and circles represent females. Horizontal lines indicate mate pairs (mother and
930 father) and vertical or slanted lines indicate parent to offspring relationship. Numbers inside
931 the symbols represent repertoire size estimates. Individuals represented by grey symbols were
932 not sequenced.

933

934



935

936

937 **Figure 3. V1R repertoire size estimates across the strepsirrhine phylogeny.** Sequences with

938 V1R homology were mined from available strepsirrhine and select outgroup genomes. Total

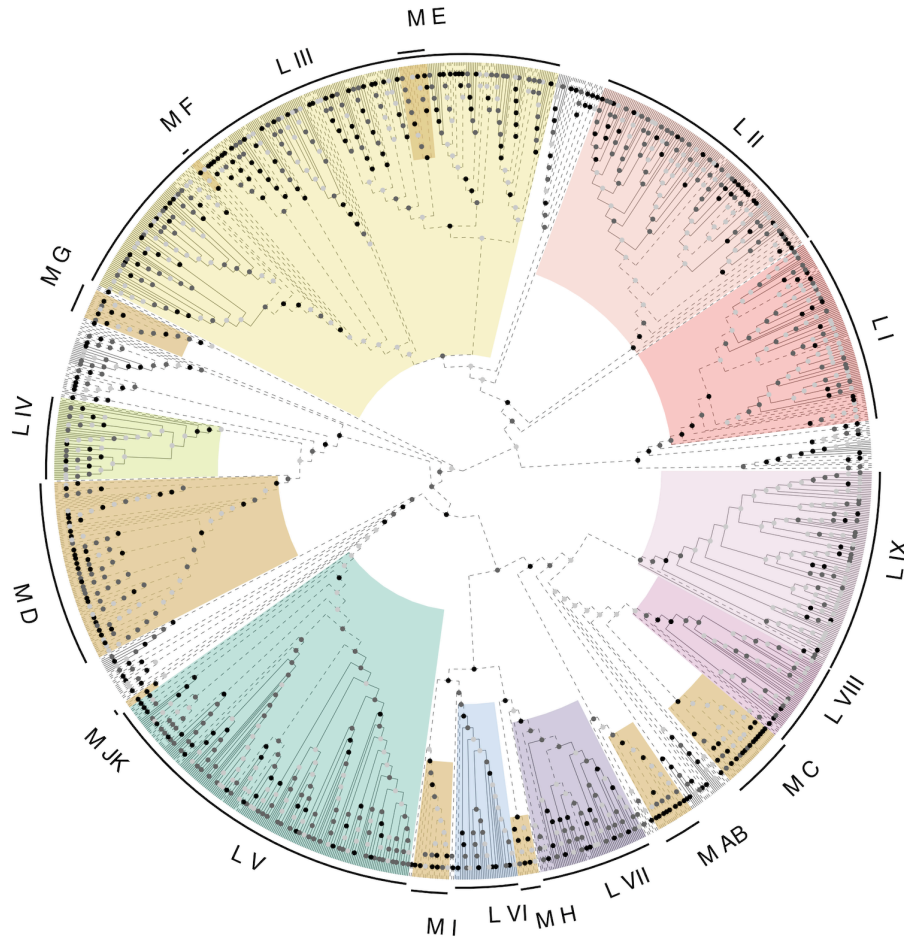
939 V1Rs consist of all genomic regions with V1R homology that are ≥ 600 bp in length. Intact genes

940 are defined by vomeronasal homology and a ≥ 801 bp ORF. Nocturnal species are highlighted in

941 gray. Tree adapted from dos Reis 2018 (dos Reis et al. 2018).

942

943



944

945 **Figure 4. ML topology of V1R repertoire.** V1R subfamilies in primates are highlighted and

946 circumscribed based on Hohenbrink et al. (2012). There are nine described subfamilies in

947 lemurs, L *Strep/I* through L IX, although not all lemur sequences fall into these subfamilies.

948 Clades of V1R subfamilies with known function in mice are shown in burnt orange (M AB

949 through M JK). Circles at nodes represent bootstrap support. Black nodes have 100% bootstrap

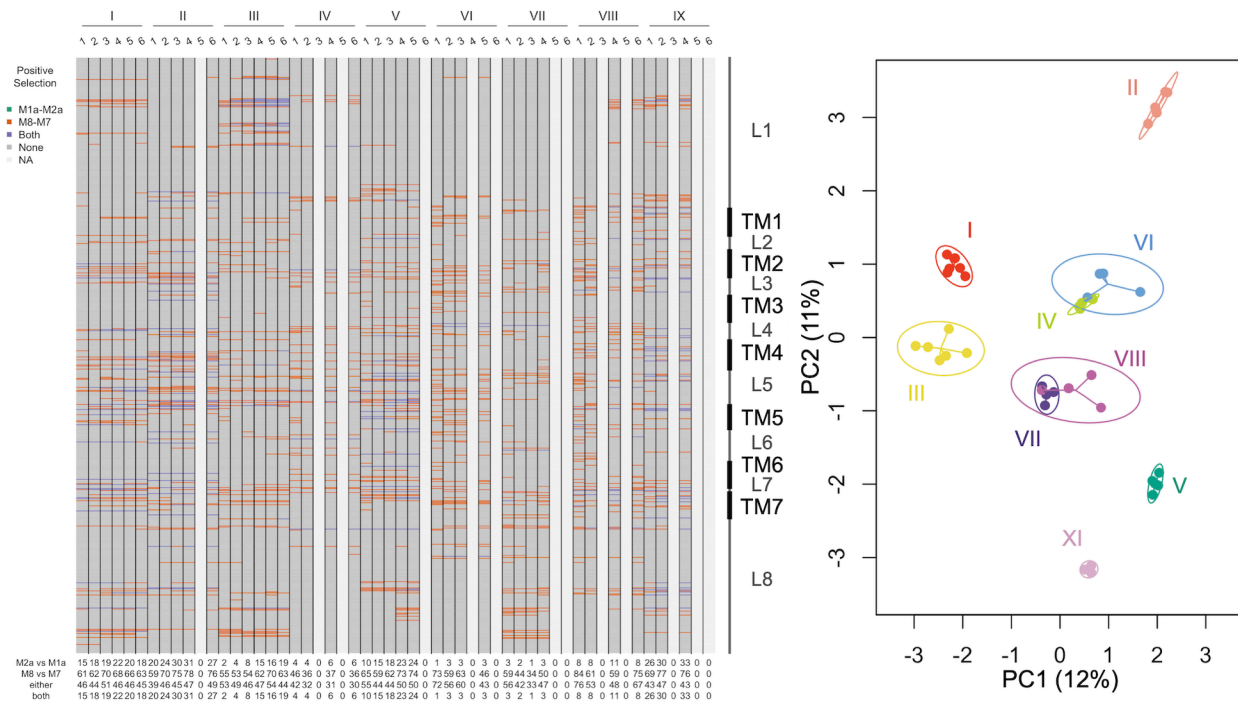
950 support, dark grey nodes are supported with 70% or more bipartitions from bootstrap trees, and

951 light grey nodes are weak or unsupported with less than 70% of bipartitions across bootstrap

952 replicates. The topology is arbitrarily rooted for visualization. Solid lines represent dwarf and

953 mouse lemur V1Rs (or branches subtending clades of dwarf and mouse lemur V1Rs). Dashed

954 lines represent V1R lineages that are not within Cheirogaleidae.



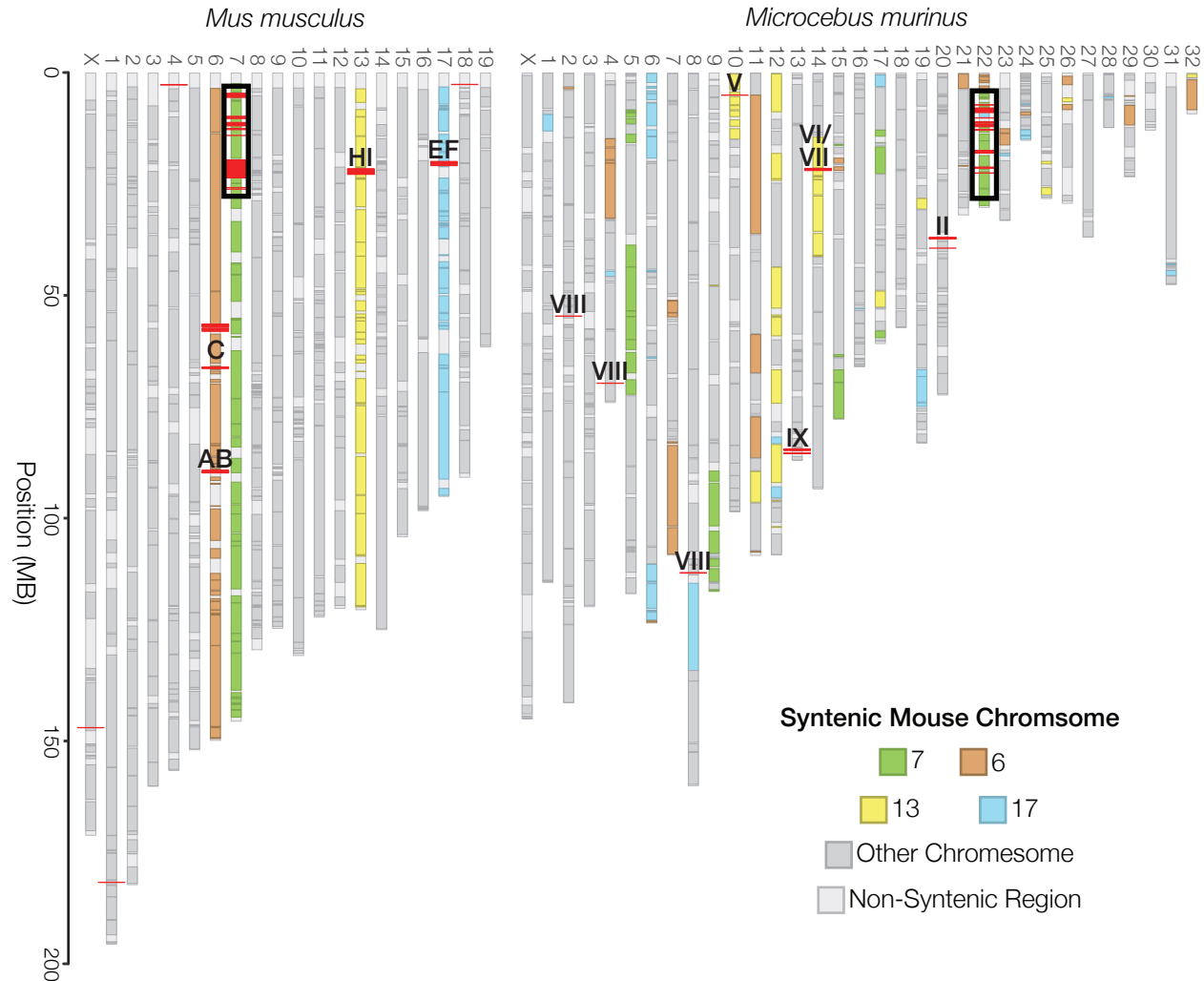
955

956

957 **Figure 5. Sites under selection across the V1R alignment.** Subfamilies are given at the top
 958 along with numbers that correspond to taxonomic filters. The first aligned codon starts at the top
 959 and the aligned codon position 588 at the bottom, with boundaries of transmembrane domains to
 960 the right. Sites under selection are colored. Missing columns means that the filter was redundant.
 961 Numbers along the bottom are counts of sites under selection detected by both model
 962 comparisons and their overlap. The boundaries of loop domains (L) and transmembrane domains
 963 (T) are shown along the aligned V1R repertoire. A PCA of sites under selection treated all
 964 codons as a binary character, determined by whether the site was under selection or not. Circle
 965 are 95% CIs for centroids of subfamily variation by taxonomic filters.

966

967



968

969

970 **Figure 6. Chromosomal synteny between mouse and mouse lemur V1R-containing regions.**

971 Synteny between *Mus musculus* and *Microcebus murinus* was estimated using the SynChro

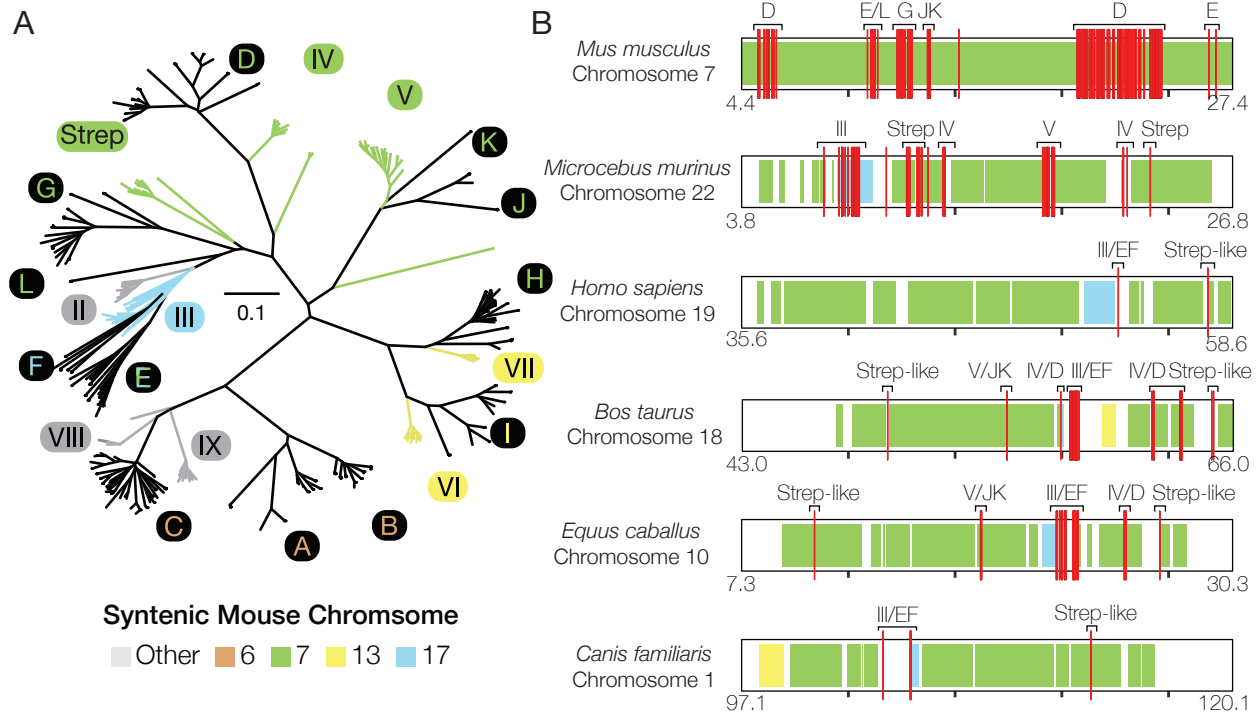
972 software. Chromosomes are colored relative to V1R-containing mouse chromosomes. V1R loci

973 are indicated with red lines and are labelled by subfamily identity. Regions outlined in black are

974 enriched for V1R loci and are examined in further detail in Figure 7B.

975

976



977

978

979 **Figure 7. Highly orthologous loci on “hotspot” V1R chromosome.** (A) RAxML tree of *Mus*
 980 *musculus* V1R cDNA sequences with intact V1R sequences from the *Microcebus murinus*
 981 genome. Mouse subfamilies are encircled in black and labelled by chromosomal location. Mouse
 982 lemur subfamilies are labelled in black and encircled in the color corresponding to the syntenic
 983 mouse chromosomal location. (B) Chromosomal “hotspot” regions enriched in V1R loci from
 984 several mammalian taxa. Orthologous regions are shaded by syntenic mouse chromosome. V1Rs
 985 loci are labelled by phylogenetic relationship to mouse/lemur subfamilies. Starting and end
 986 genomic positions are given for each species, and all regions are 23Mb long with tick marks
 987 representing 5 Mb intervals.

988

989 **Tables**

990 **Table 1. Inference of VIR birth-death process within primates.**

Node/lineage	Clade	Gains - Losses	Subfamilies Retained	Subfamilies Gained	Subfamilies Lost
Node 1	Euarchonta	NA	I, II, III, IV, VIII	NA	NA
Node 2	Primates plus Dermoptera	0 - 1	I, II, III, VIII	-	IV
Node 3	Euprimates	1 - 0	I, II, III, VIII	V	-
Node 4	Haplorrhini	0 - 2	I, III, V	-	II, VIII
Node 5	Anthropoidea	0 - 1	III, V	-	I
Node 6	Hominoidea	0 - 1	III	-	V
<i>N. leucogenys</i>	white-cheeked gibbon	1 - 1	-	VII	V
Node 7	Strepsirrhini	1 - 0	I, II, III, V, VIII	VI	-
Node 8	Lemuriformes	1 - 0	I, II, III, V, VI, VIII	IV	-
<i>D. madagascariensis</i>	aye-aye	1 - 3	III, VI, VIII	IX	I, II, V
Node 9	Lemuridae	0 - 1	I, II, III, V, VI	-	VIII
Node 10	<i>Eulemur</i>	1 - 0	I, II, III, V, VI	VII	-
Node 11	Cheirogaleidae	3 - 0	I, II, III, V, VI, VIII	IV, VII, IX	-

991

992 Note - Node numbers correspond to Figure 1. Gains and losses cannot be evaluated for Node 1

993 because it is the root node of the species tree.

994